Physics and Chemistry of the Earth 130 (2023) 103377

Contents lists available at ScienceDirect

Physics and Chemistry of the Earth

journal homepage: www.elsevier.com/locate/pce

The use of environmental magnetic properties, elemental analysis and geostatistical tools for soil pollution assessment, a lesson from Takum, Nigeria

M.O. Kanu [a,*], O.C. Meludu [b], N. Basavaiah [c], Gabriel Joseph [a]

[a] Department of Physics, Faculty of Science, Taraba State University, P.M.B. 1167, Jalingo, Nigeria
[b] Department of Physics, School of Pure and Applied Physics, Modibbo Adama University, P.M.B. 2076, Yola, Adamawa State, Nigeria
[c] Indian Institute of Geomagnetism, New Panvel, Navi-Mumbai, India

ARTICLE INFO

Keywords:
Magnetic parameters
Magnetization
Heavy metals
Pollution
Soil
Takum

ABSTRACT

The study is aimed at investigating the pollution status of Takum town, Nigeria using environmental magnetism, geochemistry and geostatistics. A total of 79 topsoil (0–10 cm) samples were collected and used for the measurement of various environmental magnetic parameters and some heavy metals (Ti, Cr, Mn, Fe, Ni, Cu, Zn, Hg and Pb). Magnetic susceptibility (χ), saturation and anhysteric remanent magnetizations were highly variable having values that ranged from 32.11 to 1118.57 $\times$ 10^{-8} m^3kg^{-1}, 95.03–1206.59 $\times$ 10^{-8} m^3kg^{-1} and 199.87–16002 $\times$ 10^{-5} Am^2kg^{-1} respectively. These values reflect top soil enhancement due to the dominance of secondary ferrimagnetic minerals which is revealed by thermomagnetic runs to be mainly magnetite. The frequency dependent susceptibility χfd% had an average value of 10.63% implying that the samples are dominated by pedogenic superparamagnetic grains. However, the presence of multi-domains grains from vehicular sources are also evident. The mean concentration of the measured heavy metals decreased in the order: Fe > Ti > Mn > Zn > Pb > Cu > Ni > Hg. Based on various indices, Hg and Pb have been identified as the elements constituting the greatest risk to the area. Significant positive correlations ($r = 0.402$, $P < 0.01$ – $r = 0.751$, $P < 0.001$) were obtained between magnetic concentration parameters and Cr, Fe, Zn, Pb and Pollution Load Index, supporting the use of environmental magnetic properties for quick assessment and monitoring of pollution levels in the Takum soils. The sources of heavy metal pollution have been identified to originate from vehicular, agricultural, pedogenic and weathering activities. Different degrees of significant correlation were obtained between magnetic parameters, heavy metals and particle size classes, indicating the possibility of using magnetic techniques as proxy for textural parameters.

1. Introduction

Environmental pollution is one amongst the numerous problems of the 21st Century. Pollutants from various activities such as agriculture, industrial waste and transportation pose threat to the environment on entry into the air, land or water bodies (Jiang et al., 2019). Since the beginning of the technology age, soil has been a repository of societal waste (Adie and Osibanjo, 2009). According to Matini et al. (2012), waste that causes environmental pollution and soil degradation is classified into four classes namely: Industrial, Agricultural, Nuclear and Municipal. Today, the state of environmental deterioration is not only associated to urban areas but also to nearby cities and towns (Taghipour et al., 2011; Naderizadeh et al., 2016; Aziz et al., 2022). This is because natural occurrences like rainfall and wind convey them from the point of their production and deposit in other locations.

To enhance the safety of life and properties in a location, it is necessary to recognize the major sources of pollution, monitor and assess the degree of such pollution in space so as to reveal its changes with time (Manisalidis et al., 2020). Examples of such pollutants are heavy metals such as cadmium (Cd), mercury (Hg), arsenic (As), chromium (Cr), Copper (Cu), Zinc (Zn), Mercury (Hg), thallium (TI) and lead (Pb). For many years, lead has been extracted from ores and used for variety of purposes and products. Lead is a primary raw material used in automobile battery. Studies show that wastes from automobile battery manufacturing companies (ABMC) are known to release a high percentage of lead on soil (Greenpeace International, 1991–1993) and these

* Corresponding author.
E-mail address: maxwell.kanu@tsuniversity.edu.ng (M.O. Kanu).

https://doi.org/10.1016/j.pce.2023.103377
Received 27 October 2022; Received in revised form 1 January 2023; Accepted 30 January 2023
Available online 31 January 2023

wastes are reported to be responsible for some of the world's most polluted sites. A survey in Kabwe a city in Zambia inhabiting about 300, 000 people revealed that it is African's most polluted city and fourth in the world (Yamada et al., 2020). This is because African's oldest lead mines of Kabwe lasted till 1994 leaving the city poisoned with high concentration of lead in the soil and water from slag heaps that were left as reminders of the smelting and mining era (Yamada et al., 2020). Evanhoe (2006) reported that lead; antimony, arsenic, copper and zinc residues left behind for more than 800 years ago still pose a potential health threat in southern France.

In a smelting plant, a by-product is formed from thermal reduction of metallic ores called slag. This term is also applied to similar materials produced in other operations like coal combustion, incineration, industrial waste sludge (Bender et al., 1998) and phosphorus production (Soodan et al., 2014). In Nigeria, slag from ABMC has been reported to contain about 6% upwards of Lead (Oyeleke et al., 2016). Contamination of the environment with heavy metals from anthropogenic sources is a major concern because of their toxicity and threat to human life and the environment (Iwegbue et al., 2006; Chen et al., 2009; Hartley et al., 2009).

In view of the detrimental effects of heavy metal pollution, there has been growing concerns on how to rapidly assess the level of pollution in the environment. Environmental magnetic techniques has been used successfully to achieve this purpose in different environments such as soils, sediment, dust etc. (Kanu et al., 2017; Yang et al., 2019; Ayoubi et al., 2020). The magnetic methods is a rapid (capable of measuring large number of samples in a short time), cost effective, sensitive and non-destructive means of assessing soil pollution by heavy metals (Karimi et al., 2011; Dankoub et al., 2012; Dong et al., 2014; Kanu et al., 2017; Ayoubi et al., 2018a, 2018b, 2019; Yang et al., 2019). This measurement is complimentary to the traditional geochemical methods and can rapidly delineate polluted spots that will be followed by measurements of point by point samples using the older methods such as Atomic Absorption Spectroscopy (AAS) etc., which are labour intensive and time consuming. The use of magnetic properties as proxy for heavy metal contamination is made possible based on the premise that magnetic particles and heavy metals originate from similar anthropogenic sources. Both parameters have strong affinity with each other. As a result, significant interrelationships have been found between magnetic particles and heavy metals, especially in sites with increased human activities (Blaha et al., 2008; Chaparro et al., 2008; Lu et al., 2010; Dong et al., 2014; Guo et al., 2015). A combination of both magnetic properties and the concentration of heavy metals will assist in the characterization of pollution in a place. Several studies have established the use of magnetic methods as a fast method of detecting pollution in Europe, America, and Asia etc. However, in Africa, such studies are scanty. There are limited data on magnetic proxy screening method of heavy metal contamination. Based on the existing literatures, such studies have not been carried out in Takum, Nigeria, This study is the first detailed application of environmental magnetism techniques for pollution assessment in the area. It adopted a multidisciplinary approach to assessing the pollution status in the town. The objectives of this work are to (i) obtain the data on magnetic parameters and the concentration of some heavy metals in the study area, (ii) further assess the use of environmental magnetic techniques to assess heavy metal pollution by correlation analysis, (iii) assess the pollution level of the study area through pollution indices and geostatistical approach, (iv) determine the sources of heavy metals and magnetic particles using multivariate statistics and (v) investigate the effect of soil particle size on the magnetic susceptibility and heavy metals.

2. Methodology

2.1. Study area

Takum is located between latitude 7° 15′ to 7° 27′ N and longitude 10° 00′ to 10° 15′ E (Fig. 1) with a total land mass of 2,500 km^2 and a population of 135, 349 based on the 2006 census figures. The mean annual temperatures in Takum ranges from 27 to 28 °C. It is a sub urban and mostly agrarian town in the southern part of Taraba State, Nigeria. As a Local Government Headquarters, it houses most of the official buildings and most government activities are performed there, thus receiving many visitors into the town. This makes it a commercial centre in the zone. Farm products such as oil palm nuts, palm oil, plantain, groundnuts and maize are produced in large quantities and sold at wholesale prices to the buyers from different parts of the country.

The town receives a mean annual rainfall of 1300 mm and characterized by the southern Guinea savannah with two different seasons: The dry season which lasts between November and March and is usually marked by the North East trade winds (harmattan) from the Sahara desert. The wet season are usually characterized by the South West winds from the Atlantic Ocean from April to early November.

The geology of Takum shown in Fig. 1 is composed of the Precambrian to upper Paleozoic Basement Complex rocks which are subdivided into undifferentiated basement, metasediment and alluvium. Towards the north, there are undifferentiated basement rocks which had been weathered and laterilized, leading to unstratified laterites, gravel, clay and silty-sands. According to Carter et al. (1963), diorite, granodiorite and migmatitic rocks are the major constituents of the uniform basement rocks. Migmatites and biotite-gneiss are also found to lie side –by –side with quarzites. There is also feldspar that contains plagioclase mixed with high percentage of kaoline and sometimes microline in form of mixtures of fine granules of quartz. The western side of Takum is dominated by the uniform metasediment rocks that has undergone metamorphosis into its constituent parts: migmatites and granites gneiss. The alluvial sediments are product of weathering from the up-hill basement rocks that are moved and laid along the bank of the river in the eastern part. They are mostly comprised of fine/medium grained sand and clay.

2.2. Method of sample collection

To assess the level of soil pollution, stratified random sampling was adopted with concentration on residential (TRA), mechanic workshop (TMV) and farmland (TFL). A total of 79 top soils (0–10 cm depth) were collected in February 2015 using a stainless steel material to avoid contamination. About 100 g of the samples were packaged in self-labelled leather bags after removing debris, stones and leaves and then transported in an air conditioned vehicle to the laboratory. The samples were air-dried for a few days, disaggregated and homogenized using agate mortar, sieved through a 2 mm sieve mesh and stored in sealed 80 cm^3 plastic containers (Fig. 2) under laboratory temperature. The samples were air lifted in April 2015 to the Environmental Magnetism laboratory, Indian Institute of Geomagnetism, Mumbai where all the laboratory measurements were performed. Samples for the routine mineral magnetic measurements were packed tightly in 8 cm^3 non-magnetic plastic containers.

2.3. Measurement of magnetic parameters

The mass specific magnetic susceptibility was measured at low (χlf = 967Hz) and high (χhf = 15,616 Hz) frequency using the MFK1-FA Kappabridge (AGICO instrument, Czech Republic). The instrument is operated using a SAFYR software within a field range of 2–700 A/M with a sensitivity of 2×10^{-8} SI. Measurements made at the two frequencies are generally used to detect the presence of fine grained <0.03 μm) super paramagnetic (SP) ferrimagnetic minerals in samples. Samples where ultrafine minerals are present will show slightly lower values at high frequency; samples without the superparamagnetic minerals will show almost the same magnetic susceptibility values at the two frequencies (Dearing et al., 1996). Frequency dependent magnetic susceptibility can be presented as either mass frequency dependent

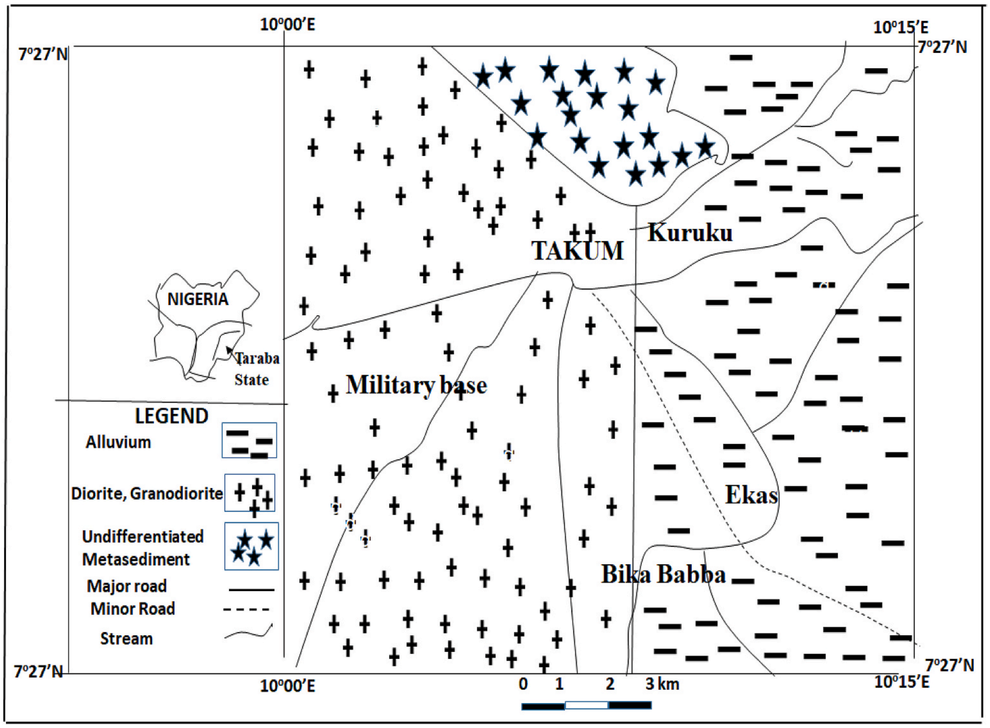

Fig. 1. Geological map of the study area (Source: Nur and Goji, 2005).

Fig. 2. Prepared soil samples packed in plastic containers.

susceptibility (χfd in m^3kg^{-1}, which is the difference between low and high frequency susceptibilities) or percentage mass specific frequency dependent susceptibility (χfd %) usually calculated using equation (1).

$$\chi fd\ (\%) = \frac{\chi lf - \chi hf}{\chi lf} \times 100 \tag{1}$$

Anhysteretic Remanent Magnetization (ARM) was acquired using the D-2000 AF demagnetizer (ASC Scientific, USA) and the remanence obtained was measured using a spinner magnetometer (Molspin ltd, UK). The acquired ARM was then converted to its susceptibility (χARM). The isothermal remanent magnetization (IRM) measurements were executed using the Molspin Pulse Magnetizer and spinner magnetometer. The samples were exposed to a forward field of 20 and 1000 mT. The 1000 mT maximum value was taken as the saturation isothermal remanent magnetization (SIRM). DC demagnetization of the SIRM (back field demagnetization) was done in steps of 20, 30, 100 and 300 mT. The data obtained was used to calculate the soft IRM, hard IRM (HIRM), S-ratio and L-ratio (equations (2)–(8)). These parameters are useful magnetic proxy parameters for interpretation of many geophysical characteristics (Oldfield, 1991; Basavaiah and Khadkikar, 2004; Basavaiah, 2012).

$$Soft\ IRM = \left(\frac{SIRM - IRM_{-30mT}}{2}\right) \tag{2}$$

$$Soft\ IRM\ (\%) = \frac{SOFT}{SIRM} \times 100\% \tag{3}$$

$$HIRM = \left(\frac{SIRM - IRM_{-300mT}}{2}\right) \tag{4}$$

$$HIRM\ (\%) = \frac{HIRM}{SIRM} \times 100\% \tag{5}$$

$$S_{100} = \frac{|IRM_{-100mT}|}{SIRM} \tag{6}$$

$$S_{300} = \frac{|IRM_{-300mT}|}{SIRM} \tag{7}$$

$$L_{ratio} = \frac{SIRM + IRM_{-300\ mT}}{SIRM + IRM_{-100\ mT}} \tag{8}$$

Some samples were selected for further magnetic analyses. Temperature dependent susceptibility (χ- T) runs were performed on three representative samples using AGICO KLY-4S Kappabridge coupled to a CS-3 furnace at 875 Hz frequency and maximum field of 300A/m. The high χ – T runs were made in an Argon environment from room temperature to 700 °C and cooled to room temperature. Hysteresis loops were produced using Princeton Corporation 2900 model Micromag Alteranating Gradient Magnetometer (AGM). The saturation magnetization (Ms), saturation remanent magnetization (Mrs), coercivity (Bc) and coercicity of remanence (Bcr) and their ratios (Mrs/Ms, Bcr/Bc) were determined.

2.4. Measurement of soil particle size

The CILAS 1064L (France) laser granulometer which measures particle sizes between 0.04 μm and 500 μm with accuracy of ±0.5% was used to measure the particle size of the soil samples. The <125 μm size fractions were used for the particle size measurement. About 200 mg of samples was scattered in the solution of sodium hexametaphosphate and emptied into the sample chamber for the 10 min duration of grain size separation. The analysis was repeated thrice per sample. Particle size analysis was carried out on 24 samples. The Wentworth (1922) classification was used to separate the different sizes thus: ≤4 μm (clay), 4–63 μm (silt), ≥63 μm (sand) and particulate matter PM 2.5 (≤2.5 μm) and PM10 (≤10 μm).

2.5. Measurement of heavy metals

The elemental analysis was carried out on 37 samples (15 from TMV, 15 from TFL and 07 from TRA) using SPECTRO XEPOS XRF spectrometer (AMATEK, Germany). The plastic containers supplied by the manufacturers were filled with about 3 g of the pulverized and homogenized samples and the torboquant powder method was selected for the XRF measurement that lasted for about 16 min. The concentrations of Ti, Cr, Mn, Fe, Ni, Cu, Zn, Hg and Pb were measured. The accuracy of the XRF measurements was determined using replicate samples, programme blanks and the certified reference materials (NIST SRM 2709), and the rate of recovery of the heavy metals were between 94 and 114%. Twelve samples constituting 32% of the total samples were measured thrice and the estimated standard errors were between 3 and 5%, and a strong positive correlation (r = 0.98–1.0) was obtained when compared with the values of certified reference materials. The Limit of Detection (LoD) determined were, Ti, Ni (1.00 mg/kg), Mn (0.40 mg/kg), Fe (0.37 mg/kg), Cu, Zn, Cr (2.0 mg/kg), Hg (0.0004 mg/kg) and Pb (2.3 mg/kg).

2.6. Assessment of the pollution indices and ecological risk

In this study, the contamination factor (CF), pollution load index (PLI), enrichment factor (EF) and the potential ecological risk index were used to assess the level of toxicity of heavy metals in the study area.

Tomlinson et al. (1980), developed an approach for assessing the level of toxicity of soil or sediment samples known as the Tomlinson Pollution Load Index (PLI). The PLI indicates the level by which the concentration of heavy metal exceeds the reference background value and provides the overall status of toxicity of a sample. According to Angulo (1996),the CF and PLI are calculated using equations (9) and (10).

$$CF_m = \frac{C_m}{C_b} \tag{9}$$

$$PLI = \sqrt[n]{(CF1 \times CF2 \times \ldots\ldots\ldots\ldots CFn)} \tag{10}$$

where C_m is the concentrations of each heavy metal and C_b the corresponding background concentration of the reference metal. It should be noted that if PLI is greater than one, the samples are polluted and results to a continuous soil deterioration due to heavy metal input (Pobi et al., 2019) and if PLI is less than one, the sample is not polluted (Barakat et al., 2012). A more detail classification of PLI has been provided by Singh et al. (1999) as follows: Background concentration (PLI = 0); unpolluted (0 < PLI ≤1); moderately to unpolluted (1 < PLI ≤2); moderately polluted (2 < PLI ≤3); moderately to highly polluted (3 < PLI ≤4); Highly polluted (4 < PLI ≤5) and very highly polluted (PLI >5). Also, the contamination factor has been classified by Hakanson (1980) into four classes as follows: Low contamination (CF < 1); moderate contamination (1 ≤ CF < 3); Considerable contamination (3 ≤ CF < 6) and very high contamination (CF ≥ 6).

The anthropogenic effect on the soils and sediments can be determined by estimating enrichment factor (EF) of heavy metals concentrations normalized with respect to the background levels (Dickinson et al., 1996). The enrichment factor could be an effective parameter for differentiating between heavy metals arising from human activities and lithogenic source and their degree of contamination. The following elements: Al, Ti, Mn, Fe, Sc or Sr could be used for normalization during EF calculation (Cai et al., 2019). Here, we calculated the EF using the equation (Cai et al., 2019):

$$EF_i = \frac{\left(C_i/C_{Fe}\right)}{\left(B_i/B_{Fe}\right)} \tag{11}$$

where C_i and C_{Fe} are the proportion of the heavy metal *i* and Fe in the samples respectively. B_i and B_{Fe} are their respective reference values of the elements i and Fe.

The reference data was taken from the Rudnick and Gao (2014) and Fe was selected as the reference or normalizing element. The selection of Fe for normalization is because of its high abundance and stability in the earth's crust. There are six grades of EF as defined by Sutherland (2000) thus: 0 < EF < 1 (no enrichment); EF < 2 (minimal enrichment); 2 < EF < 5 (moderate enrichment); 5 < EF < 20 (significant enrichment); 20 < EF < 40 (very high enrichment) and EF > 40 (extremely high enrichment).

The ecological risk of heavy metals on the study area was evaluated using the ecological risk factor (E_r^i) and the potential ecological risk index (RI) calculated following Hakanson (1980):

$$E_r^i = \sum_{i=1}^{n} T_r^i \times \frac{C_m}{C_b} \tag{12}$$

$$RI = \sum_{i=1}^{n} E_r^i \tag{13}$$

where T_r^i is the toxicity response factor for a particular metal and in this study, the following T_r^i values were used for the calculation: Ti, Mn and Zn = 1; Cr = 2; Cu, Ni, Pb = 5 and Hg = 40 Hakanson (1980); Weissmannova et al. (2019); Zao et al., 2022}. The calculated values of the ecological risk factors and ecological risk index have been grouped into various approved thresholds and groups following Hakanson (1980), Zao et al.(2022): Low ecological risk (Er < 40 and RI < 150); Moderate ecological risk (40 ≤ Er < 80 and 150 ≤ RI < 300); considerable ecological risk (80 ≤ Er < 160 and 300 ≤ RI < 600); High ecological risk (160 ≤ Er < 320); Very high ecological risk (Er ≥ 320 and 600 ≤ RI < 1200) and extremely high ecological risk (RI ≥ 1200).

2.7. Data analysis/statistical analysis

Statistical approaches such as descriptive statistics and multivariate statistics were employed for data analysis. SPSS 26, Origin 5.0, JASP 0.16.3.0 and Microsoft excel statistical softwares were used to obtain the descriptive statistics, correlation analysis and principal component analysis (PCA), boxplots and scatter plots.

3. Results and discussions

3.1. Magnetic properties of surface samples

3.1.1. Magnetic concentration parameters

The results of magnetic properties for Takum Township are summarized in Table 1. The magnetic susceptibility χ value varied widely from a value of (32.11–1118.57) × 10^{-8} m^3kg^{-1} with an average value of 103.30 × 10^{-8} m^3kg^{-1}. The average value indicates evidence of secondary ferrimagnetic minerals in the soils. The wide variation signified variable sources of enhancement in the top soil magnetic susceptibility. The strong coefficient of variation (CV %) of 149.80%

Table 1
Summary statistics of magnetic parameters from Takum.

Sample areas	Desc. Stat.	χ	χfd	χfd%	ARM	χARM	ARM/χ	χARM/χ	χARM/χfd	SIRM	χARM/SIRM	SIRM/χ	S-100	S-300	Lratio	Soft (%)	HIRM (%)
Total (n = 71)	Min	32.11	2.29	2.71	3.78	95.03	0.04	1.03	17.51	199.87	7.54	2.89	0.51	0.84	0.01	35.22	0.12
	Max	1118.57	33.42	20.23	48.01	1206.59	0.25	6.28	63.66	16002.71	171.47	14.31	0.84	1.00	0.46	64.41	8.12
	Mean	103.30	8.72	10.63	12.00	301.49	0.15	3.66	35.86	997.12	56.08	7.76	0.68	0.92	0.23	49.43	3.75
	SD	154.75	6.87	4.25	8.82	221.70	0.05	1.31	6.93	2244.59	34.56	2.45	0.08	0.04	0.11	6.70	2.12
	CV%	149.80	78.82	39.98	73.54	73.54	35.85	35.85	19.33	225.11	61.63	31.56	11.16	4.58	48.5	13.56	56.42
TRA (n = 19)	Min	42.12	2.78	5.30	4.11	118.01	0.07	1.87	30.98	199.87	23.40	4.24	0.52	0.84	0.01	39.60	0.12
	Max	83.97	12.96	18.06	16.97	426.51	0.22	5.60	43.11	672.31	20.42	8.73	0.84	1.00	0.46	63.19	7.94
	Mean	59.33	5.73	9.58	8.14	210.18	0.14	3.57	37.31	410.98	53.10	6.96	0.68	0.92	0.25	51.19	4.45
	SD	12.27	2.58	3.12	3.49	86.54	0.04	1.01	2.56	110.25	21.59	1.28	0.10	0.07	0.12	6.52	2.53
	CV%	20.67	45.01	32.53	41.18	41.18	28.36	28.36	6.86	26.83	40.67	18.46	14.46	7.39	49.69	12.73	57.00
TMV (n = 26)	Min	32.11	2.29	2.71	3.78	95.03	0.04	1.03	19.57	211.63	7.54	2.89	0.55	0.88	0.01	35.22	0.19
	Max	1118.57	33.42	20.23	48.01	1206.59	0.20	4.96	63.66	16002.71	171.47	14.31	0.82	1.00	0.42	64.41	5.90
	Mean	170.22	11.21	9.38	12.52	366.13	0.11	2.87	34.75	1916.17	47.42	9.05	0.71	0.94	0.19	46.29	2.89
	SD	237.53	10.24	5.72	13.13	328.52	0.05	1.28	10.12	3473.78	48.80	3.40	0.08	0.04	0.11	7.86	1.84
	CV%	139.54	91.32	61.01	89.73	89.73	44.62	44.62	29.12	181.29	102.92	37.61	10.84	3.91	57.07	16.98	63.87
TFL (n = 26)	Min	35.53	3.99	9.04	5.45	136.97	0.10	2.40	17.51	254.61	33.47	5.86	0.51	0.84	0.05	42.54	0.71
	Max	78.53	11.93	15.19	19.63	493.40	0.25	6.28	41.35	535.41	99.20	9.38	0.75	0.99	0.41	62.00	8.12
	Mean	63.79	8.26	12.77	12.35	299.95	0.18	4.62	36.15	441.07	67.70	6.96	0.67	0.92	0.25	51.82	4.18
	SD	10.80	2.15	1.56	4.14	95.32	0.04	0.88	4.66	68.12	17.71	0.73	0.05	0.04	0.09	4.03	1.79
	CV%	16.93	26.01	12.19	31.78	31.78	19.14	19.14	12.89	15.44	26.16	10.55	7.82	3.91	36.98	7.78	42.96

Units: χ = × 10^{-8} m^3kg^{-1}, χfd = × 10^{-8} m^3kg^{-1}, ARM = mA/m, χARM = × 10^{-8} m^3kg^{-1}, SIRM = × 10^{-5} Am^2kg^{-1}, SIRM/χ = kA/m, χARM/SIRM = × 10^{-5} m/A and others are dimensionless. Min = minimum, max = maximum, SD = standard deviation, CV = Coefficient of Variation.

calculated for the χ of all the samples indicates strong external influence. The degree of CV can be evaluated using the following classification: CV < 10% indicates weak variation, 10% ≤ CV ≤ 30% indicates moderate variation and CV > 30% indicate strong variation (Wang et al., 2017). Analysis of the results on a site specific basis indicates that the average χ values varied in the order: TMV (170.22 × 10^{-8} m^3kg^{-1}) > TFL (63.79 × 10^{-8} m^3kg^{-1}) > TRA (59.33 × 10^{-8} m^3kg^{-1}). TRA and TFL showed moderate variation (CV between 10 and 30%) between samples susceptibility, indicating less influence from external sources while the χ of the TMV samples were strongly variable (CV >30%). The average χ value of 103.30 × 10^{-8} m^3kg^{-1} obtained in all the samples from Takum, Nigeria was less than the average values obtained in road sides soil (χ = 240.53 × 10^{-8} m^3kg^{-1}) and residential areas (χ = 124.42 × 10^{-8} m^3kg^{-1}) in Jalingo Nigeria (Kanu et al., 2017, 2018). However, the average χ value of the TMV was about 24.92% higher than that obtained from Jalingo Mechanic Village (137.06 × 10^{-8} m^3kg^{-1}) by Kanu et al. (2013). This shows higher degree of pressure from human activities in the TMV. In order to assess the soil pollution level based on magnetic susceptibility, the ISO 21226 (2019) have for the first time provided the following classification based on volume susceptibility (K × 10^{-5} SI magnetic units): Low probability of pollution (0 ≥ K ≤ 30); moderate probability of pollution (30 > K ≤ 70); high probability of pollution (70 > K ≤ 100) and high pollution (K > 100). In this study, the unit of the mass susceptibility was converted to the volume susceptibility to allow for comparison with this classification. The results showed that only 1.4% of the samples (mainly from TRA) indicated low probability of pollution; 75% (22.2% from TRA, 16.7% from TMV and 36.1% from TFL) of the samples revealed moderate probability of pollution. In these areas, especially in the TFL, few control samples are required for geochemical mapping. About 6.9% and 12.5% (mainly from TMV) showed high probability of pollution and high pollution respectively. In this area regular and intense geochemical mapping is required.

The values of SIRM ranged from (199.87–16002) × 10^{-5} Am^2kg^{-1} in all the samples. Specifically, SIRM (× 10^{-5} Am^2kg^{-1}) varied from 199.87 to 672.31, 211.63–16002.71 and 254.61–535.41in TRA, TMV and TFL respectively. The χ and SIRM are generally used to denote the content of ferromagnetic/ferrimagnetic minerals having weak coercivity in samples, but χ is affected by diagenetic and paramagnetic constituents (Yang et al., 2019). The high values of χ and SIRM in the study area signifies the abundance of ferrimagnetic minerals. This is evident in the significant correlation between SIRM and χ as seen in Fig. 3a with r = 0.48, 0.66 and 0.93 (P < 0.05) for TRA, TFL and TMV respectively and r = 0.99, P < 0.001 (Table 2) for the combined data. The SIRM/χ parameter from the study area varied from 2.89 to 14.3 kAm^{-1} with an average value of 7.76 ± 2.45 kAm^{-1}, suggesting magnetite –like minerals in the soils (Van Oorschot, 2001). This value is close to the 11.3 kAm^{-1} obtained for magnetite (Wang et al., 2018) and 12.12 ± 2.18 kAm^{-1} obtained by Yang et al. (2019) for PSD magnetite in a mangrove sediments in China.

The χARM is used to estimate the proportion of single domain (SD) particles of strong ferrimagnetic minerals (e.g. magnetite and maghemite) in a sample with higher values of χARM depicting higher concentration of the ferrimagntic minerals (Verosub and Roberts, 1995) The values of χARM ranges between 95.03 and 1206.59 × 10^{-8} m^3kg^{-1} in all the samples. In the various locations, χARM varied from (118.01–426.41, average 210.18 ± 86.54) × 10^{-8} m^3kg^{-1} in TRA; (95.03–1206.59, average 366.13 ± 328.52) x 10^{-8} m^3kg^{-1}in TMV and (136.97–493.40, average, 299.95 ± 95.32) × 10^{-8} m^3kg^{-1}. The high χARM values suggests evidence of high proportion of SD magnetite in the study area. The interrelationship between χARM and χ evaluated through correlation analysis showed a good correlation with r = 0.77 at P < 0.001 (Table 2) in all the samples and r = 0.33, 0.61 and 0.70, P < 0.05 for TRA, TMV and TFL respectively (Fig. 3b). This showed clearly that the χ signal in the samples are contributed mainly by ferrimagnetic minerals in the SD (single domain) - MD (Multidomain) range with only a small contribution from paramagnetic and superparamegnetic

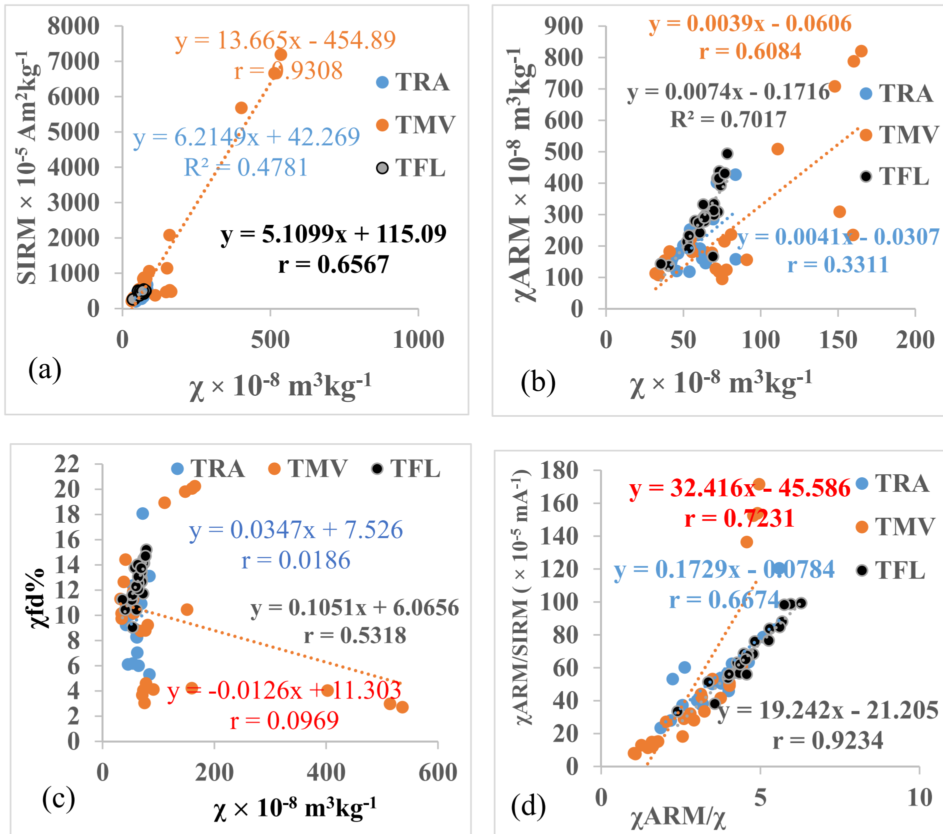

Fig. 3. Scatter plots of (a) SIRM vs. χ (b) χARM vs. χ (c) χfd% vs. χ and (d) χARM/SIRM vs. χARM/χ

Table 2
Correlation analysis between magnetic parameters from Takum.

Variable	χfd	χfd%	χ	χARM	χARM/χ	χARM/χfd	SIRM	χARM/SIRM	SIRM/χ	S-ratio	Soft IRM	HIRM	Lratio
χfd	1.00												
χfd%	**0.43c**	1.00											
χ	**0.59c**	**−0.35b**	1.00										
χARM	**0.88c**	0.18	**0.77c**	1.00									
χARM/χ	0.20	**0.87c**	**−0.39b**	0.13	1.00								
χARM/χfd	**−0.24a**	**−0.52c**	**0.24a**	0.20	−0.13	1.00							
SIRM	**0.47c**	**−0.44c**	**0.99c**	**0.69c**	**−0.43c**	**0.31a**	1.00						
χARM/SIRM	**0.57c**	**0.91c**	−0.22	**0.35b**	**0.80c**	**−0.35b**	**−0.34b**	1.00					
SIRM/χ	−0.18	**−0.80c**	**0.53c**	0.10	**−0.69c**	**0.50c**	**0.61c**	**−0.83c**	1.00				
S-ratio	−0.06	−0.22	**0.28a**	0.15	−0.22	0.11	**0.28a**	−0.15	−0.14	1.00			
Soft IRM	**0.48c**	**−0.43c**	**0.99c**	**0.70c**	**−0.42c**	**0.30a**	**1.00c**	**−0.32b**	**0.60c**	**0.28a**	1.00		
HIRM	**0.40c**	**−0.43c**	**0.80c**	**0.61c**	**−0.42c**	**0.32b**	**0.85c**	**−0.34b**	**0.66c**	−0.13	**0.84c**	1,00	
Lratio	−0.01	0.16	−0.23	−0.06	0.15	−0.07	**−0.25a**	0.12	−0.07	**0.92c**	**−0.25a**	**0.47c**	1.00

a $p < 0.05$.
b $p < 0.01$.
c $p < 0.001$.

minerals (Guda et al., 2020).

3.1.2. *Magnetic grain size dependent parameters*

The χfd%, Day plot and ratios of susceptibility and SIRM, hysteresis parameters and the day plot were used for characterizing the grain sizes of the Takum top soils. The χfd% ranged from 5.30 to 18.06% in TRA, 2.71–20.23% in TMV and 9.04–15.19% in TFL (Table 1). The mean value of χfd% in the soils of TRA (9.58%), TFL (12.77%), TMV (9.38%) and the total study area (10.63%) indicated that these soils were dominated by SP grains characteristic of pedogenic magnetic minerals (Lu et al., 2007). However, in TMV about 10 samples constituting 38% of the samples had χfd% < 5%, indicating the presence of MD magnetic grains characteristics of anthropogenic magnetite. About 15% of the TMV samples had SSD grains dominating having χfd% between 5 and 10% while the remaining 46% were completely dominated by SP grains having χfd% > 10% (Dearing et al., 1996). There was no sample in TRA and TFL that revealed the presence of MD grains. However, the presence of SSD in about 47% of the samples of TRA and 11% of TFL samples were evident. The high presence of MD grains in TMV over other sites suggests greater proportion of anthropogenic activities, principally from vehicular activities. Fossil fuel combustion has been identified as a major contributor to large MD in soils (Lu et al., 2007). The χfd% - χ plot (Fig. 3c) showed that the enhancement in the χ of TRA and TFL samples were dominated by peodegenic SP ferrimagnetic grains as they displayed positive interrelationship. However, the degree of pedogenesis is higher in the TFL samples which had r value of 0.53. In the TMV, the samples are scattered within the plot area, displaying a weak negative slope which indicate greater influence from coarse MD grains originating from pollution sources.

The χARM/χ ratio can be a helpful in quantifying the magnetic grains in the fine – coarse size fractions in magnetite dominated minerals (Verosub and Roberts, 1995). In such situation, an inverse variation between the ratio and magnetic grains is expected. It should be noted that the interpretation of the χARM/χ ratio can be difficult in samples containing significant quantity of SP or paramagnetic minerals (Van Oorschot, 2001). χARM/χ values > 8 points to small sized ferrimagnetic grains (approx. ≤ 0.1 μm) (Chaparro et al., 2017). In this study, the average values of χARM/χ were 3.57, 2.87 and 4.62 for TRA, TMV and TFL top soils, indicating the presence of large sized ferrimagnetic grains. The χARM/SIRM values ranged from 7.54 to 171.47 × 10^{-5} m/A with an average of 56.08 × 10^{-5} m/A. In the individual sites, the ratio varied from 23.40 to 120.42 × 10^{-5} m/A (average, 53.00 ± 21.59 × 10^{-5} m/A) in TRA; 7.54–171.47 × 10^{-5} m/A (average, 47.42 ± 48.80 × 10^{-5} m/A) in TMV and 33.43–89.20 × 10^{-5} m/A (average, 67.70 ± 17.71 × 10^{-5} m/A) in TFL (Table 1). The average values indicated that TMV had the lowest χARM/SIRM ratio but highly variable and the highest mean value was found in TFL but with the least variability. The level of variability of the ratio suggested that the magnetic mineral distribution of SSD grain size is higher in TMV followed by TRA and least in TFL. The χARM to SIRM ratio is mostly used as an indicator of SSD magnetic grain size which peaks at the fine SSD range and decreases as the grain size increases. (Maher, 1988). It is not affected by contributions from paramagnetic fractions. A good and significant positive correlation (r = 0.80, P < 0.001) was obtained between χARM/SIRM and χARM/χ (Fig. 3d and Table 2) in all the sites investigated. This implies that the magnetic grains sizes progressively decreased from the coarse grained SSD to finer grain sizes. The χARM/SIRM and χARM/χ are meant to minimize the magnetic concentration effects and increase the signals arising from changes in grain sizes (Liu et al., 2012).

The Dearing plot (Dearing et al., 1996) of Fig. 4a was further used to identify and get more clarifications on the grain sizes present in the Takum soils. The Dearing plot (χfd% vs. χARM/SIRM) showes that the grain sides of TMV samples is widespread across the plot area with grains sizes ranging from MD + PSD to SSD/SP transition. The TMV samples also contained 10% to >75% SP grains. MD + PSD grains were absent in the TRA and TFL soils. About 80% of the TFL samples contained >75% SP and are mostly fine SSD samples. The TRA samples contained mostly coarse SSD and fine SSD with 10–75% SP grains.

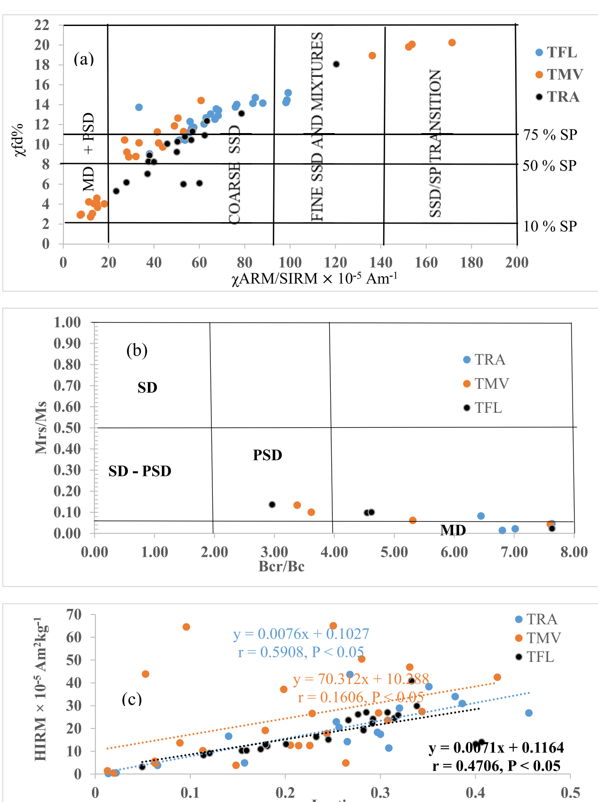

Fig. 4. (a) Dearing's plot, (b) Day plot and (c) Scatter plot of HIRM vs. L-ratio.

The presence of magnetite in the ultrafine grained sizes could be identified if SIRM/χ is greater than 40 kA/m. It should be noted that bacterial magnetite is present in the soil if χARM/SIRM is greater than 200 × 10^{-5} m/A, χARM/χ is greater than 40, and χARM/χfd greater than 1000 (Dearing et al., 1997; Van Oorschot, 2001. Based on these conditions, bacterial magnetite is likely not to play a role in the magnetic signals in Takum soils.

The results of the hysteresis parameters: saturation magnetization (Ms), remanent saturation magnetization (Mrs) and the magnetization ratio (Mrs/Ms); coercive force Bc and remanent coercive force Bcr and the corcivity ratio (Hcr/Hc) are presented in Table 3 and Fig. 4b. The value of Ms ranged from (69.02–2197.44) × 10^{-3} Am^2kg^{-1}, with a mean value of 462 × $10^{-3}Am^2kg^{-1}$. The mean value of Ms obtained in Takum top soils is close to the 480 kA/m for magnetite (Evans and Heller, 2003). The ratio of Mrs/Ms values in the study area varied between 0.01 and 0.14, with an average value of 0.07, showing that PSD particles dominate the samples. According to Evans and Heller (2003), the Mrs/Ms ratio is ≥ 0.5 for SD grains and ≤0.05 for MD particles while PSD grains are in between these values. The coercivity ratio for the Takum topsoil ranged from 2.96 to 7.63. The low value of Bc (2.22–8.44 mT with a mean of 4.78 ± 1.95 mT) obtained indicates dominance of MD grains over SD and PSD (Van Oorschot, 2001). The plot of the remanence ratio versus the coercivity ratio called the Day plot (Fig. 4b) shows that the samples are dominated by the MD and PSD particles. The hysteresis curves for selected samples are displayed in Fig. 5. The ferrimagnetic and paramagnetic fractions of the total magnetic susceptibility of the samples are also displayed. The ferrimagnetic fraction (χferri) varied between 92.58 and 99.59% while the paramagnetic component (χpara) varied between 0.41 and 7.42%, constituting a ratio of χferri to χpara of 97%:3%. This is in agreement with the χ and SIRM results. Similar results was obtained by Yang et al. (2010) for road dust in Wuhan, China. The changes in the ferrimagnetic and paramagnetic susceptibility are the cause of the variations in χferri/χpara and the estimated standard deviation could be used to identify the constant fraction (Das, 2014). The paramagnetic susceptibility in the study area were uniformly distributed over the highly variable ferrimagnetic susceptibility (Table 3).

3.1.3. Magnetic mineralogy

The following magnetic parameters were used to infer the type of magnetic minerals present in the samples: S_{-ratio} (S_{-300}), L_{-ratio}, HIRM, Soft IRM and thermomagnetic curves (χ – T curves). The S_{-ratio} is used to evaluate the relative quantity of high coercive magnetic minerals in a mixture with ferrimagnetic minerals and increases (up to a maximum of one) with increasing concentration of ferrimagnetic minerals (Kanu et al., 2017; Yang et al., 2019). S_{-ratio} decreases as hematite or goethite increases in samples. The S_{-ratio} results in the whole study area ranged from 0.84 to 1.00 (average, 0.92 ± 0.04), indicating that the samples are dominated by ferrimagnetic minerals. This is confirmed by the high soft IRM fraction, which ranged from 114.78 to 6430.18 Am^2kg^{-1} (mean, 436.28 ± 810.54 Am^2kg^{-1}). The HIRM value ranged from 0.24 to 65.03 Am^2kg^{-1} (mean, 20.70 ± 14.51 Am^2kg^{-1}). The mean ratio of soft IRM to HIRM is 49.45%: 3.75%. (Table 1). The results clearly shows the dominance of soft magnetic components like magnetite and maghemite over the hard fractions like hematite and goethite. However, the strong positive correlation between HIRM and χ (r = 0.83, P < 0.001), χARM (r = 0.61, P < 0.001), SIRM (r = 0.85, P < 0.001) and soft IRM (r = 0.84, P < 0.001) (Table 2) shows that the antiferromagnetic minerals increases

Table 3
Hysteresis parameters.

Station	Mrs (10^{-3} Am^2kg^{-1})	Ms (10^{-3} Am^2kg^{-1})	Bc (mT)	Bcr (mT)	Mrs/Ms	Bcr/Bc	χferri (%)	χparra (%)	χpara/χferri (%)
TRA 1	9.28	202.14	3.11	23.72	0.05	7.63	96.24	3.76	3.91
TRA10	30.52	2197.44	2.22	15.10	0.01	6.80	99.59	0.41	0.41
TRA 17	5.70	69.02	4.89	31.50	0.08	6.45	92.58	7.42	8.02
TRA20	6.71	310.65	2.67	18.70	0.02	7.02	98.32	1.68	1.71
TMV 8	18.29	298.26	4.89	25.94	0.06	5.31	97.96	2.04	2.08
TMV10	22.39	223.57	5.78	20.88	0.10	3.62	96.76	3.24	3.35
TMV16	8.82	202.89	3.11	23.63	0.04	7.60	96.92	3.08	3.18
TMV20	98.03	733.68	8.44	28.54	0.13	3.38	98.62	1.38	1.40
TFL 7	10.53	460.10	3.11	23.73	0.02	7.63	97.71	2.29	2.35
TFL 13	58.68	430.33	6.66	19.74	0.14	2.96	98.62	1.38	1.40
TFL 16	19.93	204.39	6.66	30.30	0.10	4.55	97.33	2.67	2.74
TFL18	21.68	216.78	5.78	26.68	0.10	4.62	97.21	2.79	2.87
Min	5.70	69.02	2.22	15.10	0.01	2.96	92.58	0.41	0.41
Max	98.03	2197.44	8.44	31.50	0.14	7.63	99.59	7.42	8.02
Mean	25.88	462.44	4.78	24.04	0.07	5.63	97.32	2.68	2.78
SD	26.97	572.77	1.95	4.89	0.04	1.77	1.76	1.76	1.92
CV%	95.95	80.74	244.68	491.84	167.04	318.46	5515.92	151.83	145.21

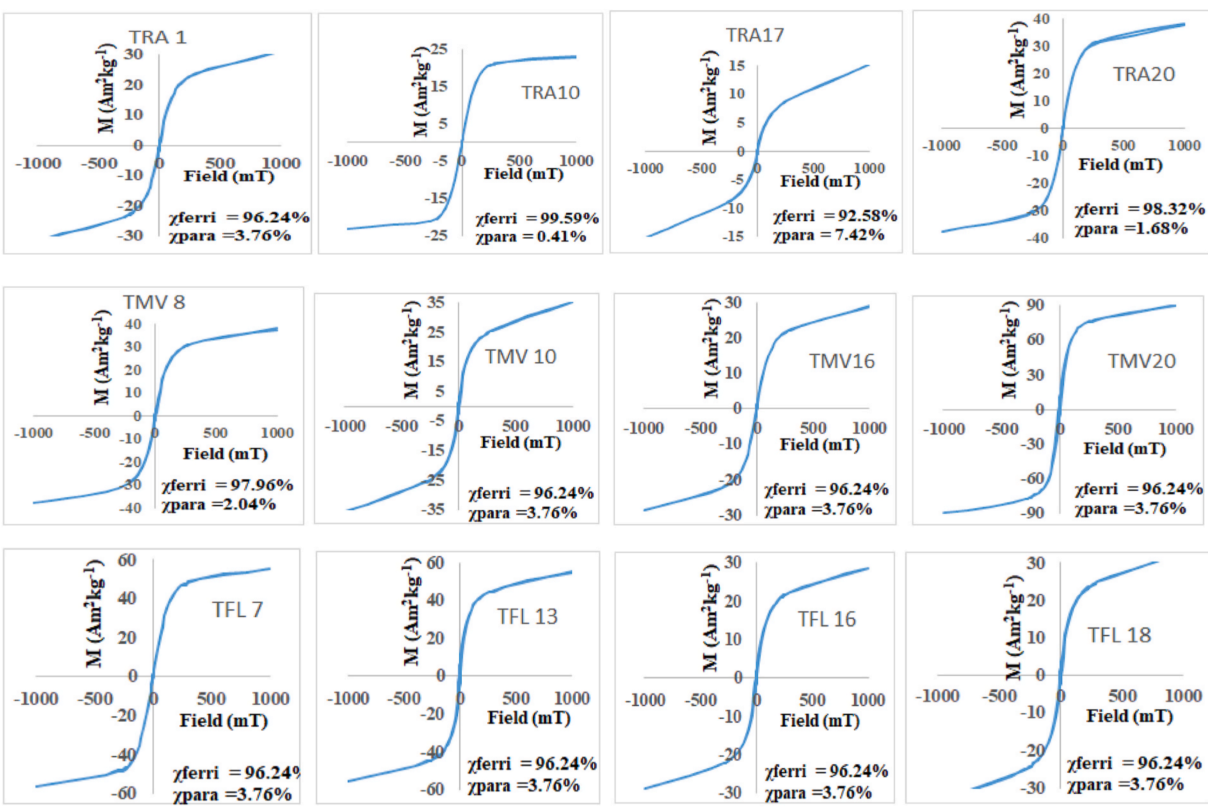

Fig. 5. Hysteresis loops of selected samples from Takum top soils. M = magnetization.

as the ferrimagnetic minerals increases. This means that both soft and hard magnetic minerals are present in the soils and they are responsible for the magnetic signals in the soils. HIRM uses coercivity values to separate magnetic signals emanating from hematite/goethite from magnetite/maghemite (Liu et al., 2012). It separates higher coercivity (hard antiferromagnetic) minerals from the soft coercive ferrimagnetic minerals in a sample, increasing with increasing values of the hard component.

L-ratio ranged between 0.01 and 0.46 with average value of 0.23 ± 0.11 in the study area. L–ratio is used to determine the extent to which the hematite hardness influences HIRM and S-ratio (Liu et al., 2012). Conventional interpretation of HIRM and S-ratio is made easy if the L-ratio is stable. Variability in the values of L-ratio reflects changes in the high coercivity distribution. In the present study, the coefficient of variation (CV) of L-ratio indicates that TMV (CV = 57.07%) > TRA (CV = 49.69%) > TFL (CV = 36.98%). This implied that the distribution in hematite or goethite is higher in TMV than other sites. This outcome is also reflected in the good linear covariation between HIRM and L-ratio in TRA ($r = 0.59$, $P < 0.05$) and TFL ($r = 0.47$, $P < 0.05$) but not in TMV ($r = 0.16$, $P < 0.05$) (Fig. 4c). The good interrelationship between HIRM and L-ratio in TRA and TFL signified that the coercivity mainly controls the HIRM instead of antiferromagnetic minerals. The differences in the degree of correlation could also point to the differences in quantity of hematite or goethite, characterizing the varying sources during soil formation (Liu et al., 2007). In Table 2, considering the entire study area, L-ratio has a weak negative correlation with some magnetic concentration parameters (χ, SIRM and soft IRMs) with $r = -0.23$, -0.25 and -0.25 at $P < 0.05$ respectively, and strong positive correlation with

HIRM (r = 0.47, P < 0.001) and S-ratio (r = 0.92, P < 0.001). The overall positive correlation Between HIRM and L-ratio is a confirmation that high coercive minerals (e.g. hematite and goethite) are present in the soil. It was therefore concluded that, although, there exist a certain quantity of antiferromanetic minerals in the samples (with more in TRA and TFL), the ferrimagnetic minerals dominates in the Takum soil.

The thermomagnetic (χ-T) curves for three representative samples presented in Fig. 6 revealed that magnetite dominated the samples as the Curie point temperature of approximately 580 °C was attained. The dominance of MD magnetite is also demonstrated by the sharp drop of χ (especially in sample TMV 8) during the heating runs close to the Curie point temperature. During the heating process, mineral alterations between 300 °C to 400 °C were observed in all the curves. This attest to the presence of titanomagnetite in the samples (Liu et al., 2012). Also, the susceptibility of the cooling curves were higher than that of the heating curves, indicating that new ferrimagnetic mineral (magnetite) were formed in the process.

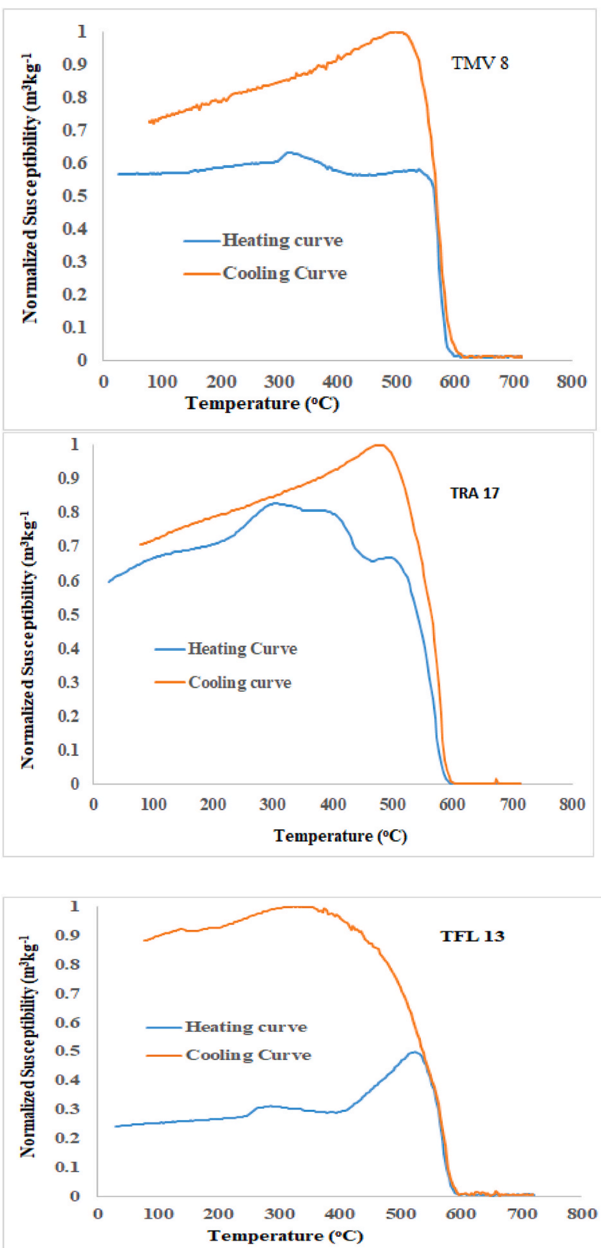

Fig. 6. Thermomagnetic curves of representative samplesThermomagnetic curves of representative samples.

3.2. Elemental concentration in Takum topsoil

The results of concentration of Ti, Cr, Mn, Fe, Ni, Cu, Zn, Hg and Pb in soil samples from Takum town are presented in Table 4. The mean concentration (in mg/kg) of these metals are in the order Fe (16,514.2) > Ti (8057.4) > Mn (482.9) > Zn (89.9) > Pb(36.4) > Cr (18.4) > Cu (14.9) > Ni (13.4) > Hg (1.0). This pattern was observed in the various sites with minor discrepancies. For example, in TFL, Cu > Ni > Cr and in TRA, Ni > Cu > Cr. The calculated coefficient of variation indicates that all the elements had strong coefficient of variation (CV > 30%) except Pb which had moderate coefficient of variation (10% < CV < 30%). Zn is most variable, followed by Cu, Cr, Ni, Fe, Hg, Ti, Mn and Pb, highlighting the degree of external influence. The heterogeneous distribution of Zn and Cu (which had CV values of over 100%) is noted and their concentrations might come from both local (point) sources of pollution and external (non-point) sources. It was further observed that the average concentration of Ti, Zn Hg and Pb exceeded the geochemical background (upper continental crust) values according to Rudnick and Gao (2014) by 2.6, 1.3, 20.0 and 2.1 times respectively. This shows these elements might have been influenced by anthropogenic sources from vehicular, agricultural or other human activities. Similar results were obtained by Ayoubi et al. (2018 2018b, 2019). The distribution of the average values of Ti, Zn and Pb in the three sampling sites are in the order TMV > TFL > TRA but Hg displays a different order of TFL = TRA > TMV.

Titanium is vastly distributed and highly abundant occupying the 9th position in the earth's crust. It is mostly present in soils and sediments as an end product of weathering, fossil fuel consumption fallout, incineration of wastes containing Titanium (WHO, 1982). The use of TiO_2 as whitening pigments in plastics, paints, enamels and cosmetics and in industries engaged in electrical dyeing may add to the Ti content in soils. It may also be from high application of Ti- containing fertilizers. It should be noted that Ti and its compounds does not pose any health risk since it is not a vital element in animals and man. However, higher degree of exposures may cause little changes in lungs. If Ti dust is inhaled, it may cause chest stiffness and pain, cough and difficulties in breathe taking (WHO, 1982). Irritation may also results if the skin and eyes gets in contact with Ti. For plants, Ti is useful for their growth and general performance when applied at small amount through their roots or leaves (Lyu et al., 2017). Crop production has been improved when fertilizers enriched with Ti (e.g. Tytanit) are applied in soils (Lyu et al., 2017). Zinc is an essential nutrient in man and its deficiency may results in birth defects, anorexia, retardation in growth, poor healing of wound etc. while excess Zn causes vascular shock, nausea, vomiting, pancreatitis and diarrhoea (WHO, 1982). In soils, it occurs either naturally or through anthropogenic deposition such as coal, waste burning, mining, steel processing, wear and tear of car tires, brake linings (Naderizadeh et al., 2016). Mercury is among the highly toxic element and is considered a global pollutant (Teng et al., 2020). It can enter the soil through industrial activities, combustion of fossil fuels, waste discharge, mining of Hg, forest fires, fertilizers containing mercury and pesticides (Teng et al., 2020). Lead can be generated from combustion of vehicle fuels, brake linings, wear of tires and leaded paints. It is a good indicator of pollution generated from traffic.

It should also be noted that although the average concentrations of Cr, Mn, Fe, Ni and Cu were less than the background values, the individual concentrations of these elements in some of the samples were higher than the background concentration. For example, the background concentration of Mn were exceeded by 7% of the samples in TMV, 14% in TFL and 22% in TRA. About 36% of TMV samples exceeded the background value of Fe and 21% were in excess of Cu background value. Comparing the results of the present study with other studies in Nigeria, it was observed that, in the residential areas, the elemental concentration in Takum is greater than that of Jalingo (Kanu et al., 2018). Similarly, elemental concentrations in Takum mechanic village and Farmland were higher than in Illorin, Nigeria (Oruson et al., 2020)

Table 4
Descriptive Statistics of Geochemical Parameters (in mg/kg) of Takum Top soils and comparison with background values and other studies.

locations	Stat	Ti	Cr	Mn	Fe	Ni	Cu	Zn	Hg	Pb
All (n = 37)	Min	2810.0	1.0	214.5	6116.0	3.9	2.8	11.5	0.3	15.4
	Max	16490.0	64.6	842.5	43520.0	44.9	86.9	457.5	2.3	66.9
	Mean	8057.4	18.4	482.9	16514.2	13.4	14.9	89.9	1.0	36.4
	SD	2856.5	17.4	146.8	10426.5	9.4	15.4	96.1	0.4	9.9
	CV%	35.5	94.5	30.4	63.1	69.9	103.0	106.9	39.8	27.2
TMV (n = 15)	Min	2810	10.5	214.5	6116.0	5.7	2.8	11.5	0.3	15.4
	Max	16490	64.6	842.5	43520.0	35.3	86.9	457.5	1.5	66.9
	Mean	9019.1	35.0	554.3	25179.8	18.9	24.1	113.3	0.9	37.5
	SD	3824.2	17.4	184.0	11921.7	9.0	21.6	139.0	0.3	15.2
	CV%	42.4	49.6	33.2	47.3	47.7	89.3	122.7	38.8	40.6
TFL (n = 15)	Min	4134	1.0	343.4	8531.0	6.1	4.9	21.7	0.5	32.5
	Max	9574	17.2	587.1	14330.0	12.9	27.9	209	1.5	44
	Mean	7991.5	8.7	455.1	10929.9	8.8	9.8	68.9	1.1	36.4
	SD	1746.9	4.5	69.6	1901.7	1.9	5.6	46.9	0.3	4.3
	CV%	21.9	51.4	15.3	17.4	22.0	57.3	68.1	28.1	11.7
TRA (n = 07)	Min	4512	1.0	252.3	7153.0	3.9	4.2	14.1	0.4	25.9
	Max	10320	27.9	666.2	25820.0	44.9	15.3	218.4	2.3	44.6
	Mean	6663.9	7.9	414.9	11721.1	12.1	8.5	86.1	1.1	34.8
	SD	2045.2	8.3	136.5	6367.3	12.9	3.9	69.7	0.6	5.7
	CV%	30.7	105.6	32.9	54.3.0	106.7	46.0	80.9	50.1	16.3
Background values[a]		3117	92	527	30890	47	28	67	0.05	17
Residential area[b]		5357.9	6.4	318.8	9991.2	7.0	6.5	61.9	0.8	47.2
Automobile workshop[c]		–	108.2	66.69	377.73	–	22.6	15.19	–	28.65
Farmland[d]		–	7.52	–	22.21	5.31	–	–	–	6.80

[a] Upper continental crust values after Rudnick and Gao (2014).
[b] Kanu et al. (2018).
[c] Oruson et al. (2020)
[d] Iyama et al. (2022).

and Port Harcourt, Nigeria (Iyama et al., 2022) respectively.

3.3. Assessment of heavy metal contamination using pollution indices

The impact of the contribution of human activities to the concentration of elements in their natural state in the Takum urban top soil was assessed using a number of indices: Contamination Factor (CF), Pollution Load Index (PLI) and Enrichment Factor (EF) while the elemental impact on the ecosystem was analysed using Ecological Risk Factor (E_r^i) and Ecological Risk Index (RI). The descriptive statistics of contamination factor CF PLI, EF and Er are summarized in Whiskers boxplots (Fig. 7). The range and mean values of the estimated CF are as follows: Hg: (6.00–46.00 and mean, 20.49 ± 8.16) > Ti: (0.90–5.29, mean, 2.59 ± 0.92) > Pb: (0.91–1.65, mean, 2.14 ± 0.58) > Zn: (0.17–6.83, mean, 1.34 ± 1.44) > Mn: (0.41–1.60, mean, 0.92 ± 0.28) > Fe:(0.20–1.41, mean, 0.54 ± 0.34) > Cu: (0.10–3.10, mean, 0.53 ± 0.55) > Ni: (0.08–0.96, mean, 0.29 ± 0.30) > Cr: (0.01–0.70, mean, 0.20 ± 0.19). Using the classification of Hakanson (1980), Mn, Fe, Cu, Ni and Cr had mean CF < 1, implying low contamination while Zn, Pb and Ti had mean CF value between 1 and 3 which indicates moderate contamination of the soils by these heavy metals. Hg had mean CF > 6 suggesting very high contamination. There are however some exceptions on the CF classification based on the mean values. For example, about 9 samples (24%) had values between 3 and 6 indicating considerable contamination. Also, 14% samples of Fe had CF values between 1 and 3, an indication of moderate contamination of the soils by Fe.

The total toxicity status of the soils can be assessed by the pollution load index (PLI) and in this study, it has a range of 0.44–1.65 with average value of 0.97 ± 0.37. The mean value shows that the soils are not polluted. However, 15 samples, constituting 41% had PLI value between 1 and 2, signifying moderately to unpolluted samples (Singh et al., 1999).

The range and mean values of the calculated enrichment factor (EF) results are as follows: Ti: 0.81–13.92 (6.17 ± 2.91), Cr: 0.04–0.86 (0.33 ± 0.18), Mn: 0.60 – 3-92 (2.08 ± 0.73), Ni: 0.21–2.56 (0.58 ± 0.37), Cu: 0.37–4.18 (0.98 ± 0.67), Zn: 0.51–8.74 (2.70 ± 2.10), Hg: 8.09–146.83 (52.17 ± 31.25) and Pb: 1.81–8.77 (5.07 ± 2.10). The mean values displayed variable enrichment of the soils. Cr, Ni and Cu were not enriched in the soils since their values falls within the classification 0 < EF < 1 (Sutherland, 2000). Mn and Zn were moderately enriched in the soil, having EF value in the range: 2 < EF < 5. The EF values of Ti and Pb were between 5 and 20 which implied significant enrichment. The EF value of Hg was >40, indicating extremely high enrichment. There were minor differences between samples. For example, from the EF values of Ti, about 12% of the samples are moderately enriched while 5% of the samples are not enriched. The EF for Mn indicated that 30% of the samples show minimal enrichment. Similarly, EF value for Zn showed that 26% of the samples are not enriched, 22% are moderately enriched and 8% are significantly enriched. Pb EF values indicate that 14% of the samples are minimally enriched while 27% are moderately enriched. In all cases, there is evidence of anthropogenic influence in the concentration of Mn, Zn, Ti, Pb and Hg, but Ti, Pb and Hg are elements most likely to cause threat to the environment and human health.

The ecological risk factor (E_r^i) calculated for the Takum soils is shown in Fig. 7. The minimum – maximum and mean values of the E_r^i are as follows: Ti (0.90–5.29, mean, 2.58 ± 0.92), Cr (0.02–1.40, mean, 0.40 ± 0.38), Mn (0.41–1.60, mean, 0.92 ± 0.28), Ni (0.41–4.78, mean, 1.43 ± 1.00), Cu (0.50–15.52, mean, 2.67 ± 2.74), Zn (0.17–6.83, mean, 1.34 ± 1.43), Hg (250.00–1840.00, mean, 819.46 ± 326.27) and Pb (4.53–19.68, mean, 10.72 ± 2.92). This implied that the decreasing order of the E_r^i are Hg > Pb > Cu > Ti > Ni > Zn > Mn > Cr. Based on the Zao et al. (2022) classification, it was found that Ti, Cr, Mn, Ni, Cu, Zn and Pb have E_r^i < 40, indicating low ecological risk with mercury as the only metal exhibiting very high ecological risk (E_r^i > 320). Potential ecological risk index (RI) followed similar trend as the E_r^i with Hg having the highest value while Cr had the lowest value. In the different sites, the mean E_r^i values indicates that TRA (906.67) > TFL (902.86) > TMV (680.00). The ecological risk index (RI) values are as follows, Hg (30, 320.00) > Pb (396.47) > Cu (98.64) > Ti (95.64) > Ni (53.79) > Zn (49.63) > Mn (33.90) > Cr (14.84). The highest estimated RI for Hg can be interpreted as extremely high ecological risk. This is followed by Pb

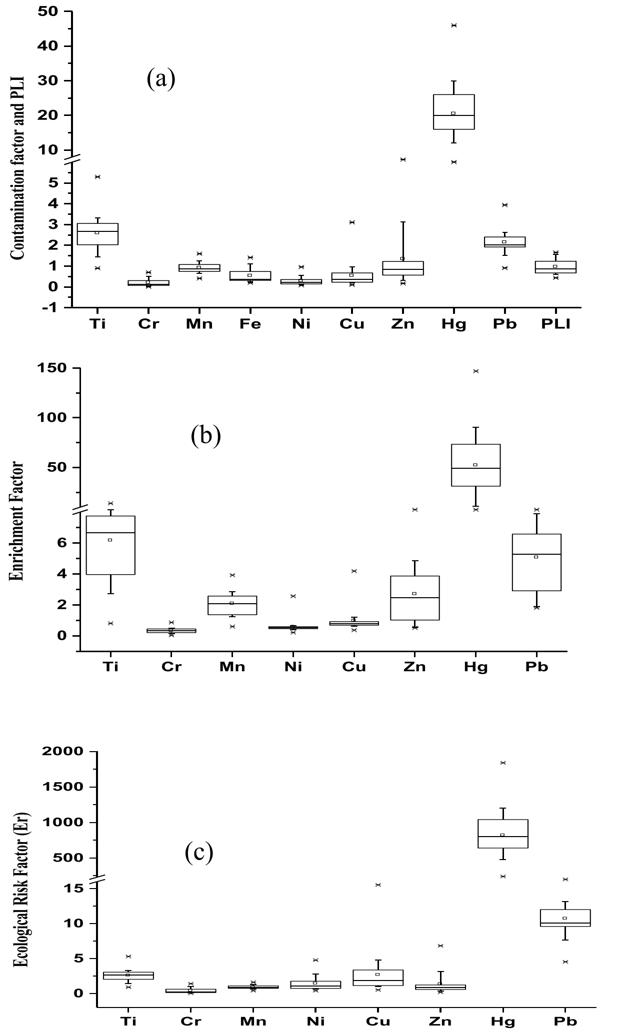

Fig. 7. Pollution indices: (a) Contamination factor and pollution load index (b) enrichment factor and (c) ecological risk factor.

with RI value between 300 and 600 implying considerable ecological risk. Other elements have Ri < 150 and are said to pose low ecological risk. The High ecological risk and toxicity for Hg calls for concern and further research on this element in the study area should be carried out

3.4. Relationship between Takum magnetic and geochemical parameters

The results of correlation analysis between magnetic and geochemical parameters from Takum soils samples are presented in Table 6. Correlation statistics (Pearson) was required to further access the source of magnetic signals and geochemical concentrations within Takum soil. Correlation analysis was also used to assess the feasibility of using magnetic methods as proxy for geochemical concentration in Takum soils. Strong positive significant correlations are found between χ and Cr (r = 0.646, P < 0.001), Fe (r = 0.636, P < 0.001), Cu (r = 0.767, P < 0.001), Zn (r = 0.679, P < 0.01) and PLI (r = 0.635, P < 0.001), suggesting that these metals are of anthropogenic origin. SIRM and soft IRM also displayed varying degrees of significant correlation with Cr, Fe, Cu, Zn, Pb and PLI but moderate negative correlation with Hg. In addition to Cr, Fe, Cu, Zn, Pb and PLI, χARM displayed strong positive correlation with Mn (r = 0.517, P < 0.001) and Ni (r = 0.519, P < 0.001). HIRM which reflects the concentration of hard antiferromagnetic minerals in samples display significant positive correlation with Fe (r = 0.357, P < 0.05), Cu (r = 0.817, P < 0.001), Zn (r = 0.440, P < 0.01), Pb (r = 0.687, P < 0.001) and PLI (r = 0.468, P < 0.01). It is evident from the results that increase in magnetic concentration properties (χ, χARM, SIRM, soft IRM and HIRM) are proportional to the enrichment of heavy metals, particularly, Cr, Fe, Cu, Zn and Pb. The strong positive correlation indicates that the magnetic concentration and elemental parameters coexist and originate from a similar source, mostly anthropogenic (Wang et al., 2018). This gives credence to the use of magnetic concentration dependent parameters as proxy parameters for the concentration of these elements. However, χARM is observed to have the highest correlation coefficient and may be the best indicator for heavy metal pollution monitoring in Takum soils. The correlation results for the grain size-proxy parameters: χfd%, SIRM/χ and χARM/SIRM shows that χfd% has moderate positive correlation with Ti (r = 0.454, P < 0.01), Mn (r = 0.510, P < 0.01), Ni (r = 0.398, P < 0.05), and negatively interrelated with Zn (r = - 0.527, P < 0.001) and Pb (r = 0.336, P < 0.05). This implies that Ti, Mn and Ni are from geogenic or crustal sources while Zn and Pb are of anthropogenic origin. SIRM/χ correlate positively with Cu, Zn and Pb while χARM/SIRM correlate positively with Cr, Mn, Fe and Ni and negatively with Zn. A prominent observation in the magnetic – elemental linkage is that the PLI only vary significantly with the magnetic concentration – dependent parameters, supporting their use for pollution assessment. It should be noted that variation in the degree of correlation is as a result of the different response of the magnetic signals to the different sources of heavy metal pollution in the study area. To isolate the various sources of metal pollution, the principal component analysis was used.

3.5. Principal component analysis (PCA) and the path diagram of Takum data

The magnetic and elemental data sets were subjected to PCA analysis in order to further delineate their likely sources in the soil. By applying variamax rotation and Kaiser Normalization, four principal components were extracted with total cumulative variance of 82.30%. The data sets

Table 6
Correlation between magnetic and elemental concentration in Takum soils (n = 37).

Variable	χfd	χfd%	χ	χARM	SIRM	SIRM/χ	Soft IRM	HIRM	χARM/SIRM
Ti	0.248	**0.454**[b]	−0.125	0.123	−0.183	−0.180	−0.186	−0.032	0.301
Cr	**0.674**[c]	0.121	**0.646**[c]	**0.683**[c]	**0.491**[b]	0.111	**0.494**[b]	0.311	**0.330**[a]
Mn	**0.692**[c]	**0.510**[b]	0.203	**0.517**[b]	0.019	−0.240	0.028	0.108	**0.565**[c]
Fe	**0.697**[c]	0.140	**0.636**[c]	**0.689**[c]	**0.471**[b]	0.097	**0.473**[b]	**0.357**[a]	**0.351**[a]
Ni	**0.675**[c]	**0.398**[a]	0.259	**0.519**[c]	0.077	−0.213	0.084	0.134	**0.516**[b]
Cu	**0.410**[a]	−0.253	**0.767**[c]	**0.712**[c]	**0.745**[c]	**0.501**[b]	**0.744**[c]	**0.817**[c]	−0.084
Zn	−0.018	**−0.527**[c]	**0.679**[c]	**0.340**[a]	**0.751**[c]	**0.663**[c]	**0.749**[c]	**0.440**[b]	**−0.409**[a]
Hg	−0.070	0.217	−0.316	−0.194	**−0.331**[a]	−0.237	**−0.332**[a]	−0.234	0.119
Pb	0.138	**−0.336**[a]	**0.512**[b]	**0.402**[a]	**0.548**[c]	**0.516**[b]	**0.545**[c]	**0.687**[c]	−0.183
PLI	**0.674**[c]	0.089	**0.635**[c]	**0.705**[c]	**0.515**[b]	0.231	**0.518**[b]	**0.468**[b]	0.256

[a] p < 0.05.
[b] p < 0.01.
[c] p < 0.001.

were well represented as indicated by the communalities which ranged from Hg (47.9%) to χARM (98.2%) (Table 8). In the first principal component, PC1, close association was found between χ, χARM, SIRM, soft IRM, HIRM, Cu, Zn and Pb (Table 8) which explained over 32.56% of the total variance extracted. This may indicate elements of anthropogenic origin majorly from vehicular and agricultural sources. The close association between these metals (Cu, Zn and Pb) and the magnetic concentration parameters in this PC gives a strong indication of anthropogenic origin and most likely the dominant influencing source of pollution in the Takum soil. This is further supported by the fact that the PC accounted for most of the variability in the data. Zn and Pb and some percentage (21%) of Cu in TMV has been noted to have values above the background. Also, the estimated EF values showed that Zn is moderately enriched while Pb has undergone significant enrichment in the soil. The Zn in the Takum soil might have originated from pesticide and fertilizer applied in the farms. Moreover, Zn and its compounds are utilized in the manufacture of fertilizers for agricultural purposes. Zn may also come from car tire wear and tear and corrosion of galvanised metal parts. Cu is used as a necessary ingredient in livestock feeds. It can be converted to animal manure and applied in the farms (Zhang et al., 2012). Cu accumulation in soil can also result from the use of pesticides (Jiang et al., 2019). Furthermore, it should be noted that local farmers usually apply either fertilizer or pesticides without knowledge of the recommended quantity. That is to say expert's advice is not sought in most instances. This could lead to high concentration of the metals in the soil. Pb enhancement in the soil is linked to vehicular and traffic waste deposition and as additive in paints (Kanu et al., 2017) and lead accumulators. Zn, Cu and Pb are also found in municipal waste.

The second PC (PC 2) is comprised of χfd, Cr, Mn. Fe and Ni and explains 20.87% of the total variance. These elements might be attributed to pedogenic or geogenic origin. The third PC (PC 3) constitutes 19.67% of the total variance and consisted of χfd, χfd%, χARM/χ, χARM/SIRM and SIRM/χ. These are mostly grain size magnetic parameters. Note that χfd appeared in two PCs contributing 66.2% to PC2 and 64.7% to PC3. In PC 2, the χfd parameter acted as concentration parameter describing the pedogenic and/or weathering origin of the elements and in PC 3, it performed the role of grain size parameter. PC 4 had Ti and Hg as the only members and constitutes 9.20% of the total explained variance and may originate from both natural and human activities. Ti is one of the most abundant element in the earth's crust occupying the 9th position and its presence in the Takum soil is likely due to weathering and erosion processes. However, the anthropogenic input through fossil fuel consumption fallout, refuse dumps incineration and Ti containing fertilizers cannot be ruled out. It should be noted that the concentration of Ti was about 2.6 times higher than the background value and the enrichment factor estimation indicated significant enrichment of Ti in the soils. Similarly, the fact that Hg content was 20 times higher than the background value and extremely enriched in the soil (based on EF calculation) attests to its anthropogenic origin. In this case, it is suspected to emanate from forest fires, fertilizers and pesticides containing Hg and waste discharge.

In order to confirm the PCA results and establish the interrelation and sources of magnetic and geochemical variables, the path diagram was constructed (Fig. 8). The path diagram is a pictorial categorization of the variables into clusters based on the assumed sources. The intensity of covariation is shown by arrows moving from the variables to the principal components. The wider the arrow, the higher the strength of covariation. Arrows may be red or green depending on whether the loadings on the PC are negative or positive. In Fig. 8, four PCs are clearly differentiated coinciding with the number of PCs obtained from the PCA. Generally, the anthropogenic sources of pollution in the study area originated from vehicular emissions from automobile exhausts pipes, condemn oils, brake linings and wear and tear of car tires, rusted pieces of metals, cement or concrete materials used for road and gutter construction, waste dumps and paints. Also, there could be inputs from organic and inorganic fertilizers, pesticides and herbicides.

3.6. *Soil textural properties and its relationship with magnetic and geochemical parameters*

Further probe into the soil texture of the top soil of the study area showed that the silt (52.36%) fraction dominated the samples. This was followed by sand (38.30%) and clay (9.84%) fractions respectively

Table 8
Results of Extracted Principal Components (PCs) analysed for Takum urban soils. The values in bold font indicate significant square loadings of variables to the respective PCs. Only PC loadings >0.6 is considered.

Variable	Principal Components				Communality
	1	2	3	4	
χfd	0.279	**0.662**	**0.647**	−0.008	0.935
χfd%	−0.329	0.323	**0.804**	0.269	0.931
χ	**0.890**	0.250	0.038	−0.295	0.943
χARM	**0.718**	0.441	0.515	−0.080	0.982
χARM/χ	−0.218	0.011	**0.798**	0.346	0.804
SIRM	**0.915**	0.063	−0.163	−0.275	0.943
χARM/SIRM	−0.218	0.469	**0.834**	0.077	0.968
SIRM/χ	0.588	−0.130	**−0.734**	−0.021	0.901
Soft IRM	**0.916**	0.065	−0.136	−0.283	0.943
HIRM	**0.792**	0.133	−0.324	0.145	0.771
Ti	−0.068	0.301	0.166	**0.750**	0.685
Cr	0.384	**0.811**	0.071	−0.271	0.883
Mn	0.107	**0.764**	0.264	0.312	0.762
Fe	0.403	**0.828**	0.070	−0.180	0.886
Ni	0.086	**0.809**	0.185	0.101	0.707
Cu	**0.850**	0.344	−0.113	0.064	0.858
Zn	**0.640**	0.165	−0.375	−0.326	0.684
Hg	−0.157	−0.210	0.151	**0.623**	0.479
Pb	**0.676**	0.202	−0.263	0.080	0.935
Eigenvalue	6.186	3.9656	3.737	1.748	
% Variance	32.559	20.871	19.667	9.203	
% Cumulative Variance	32.559	53.430	73.097	82.299	

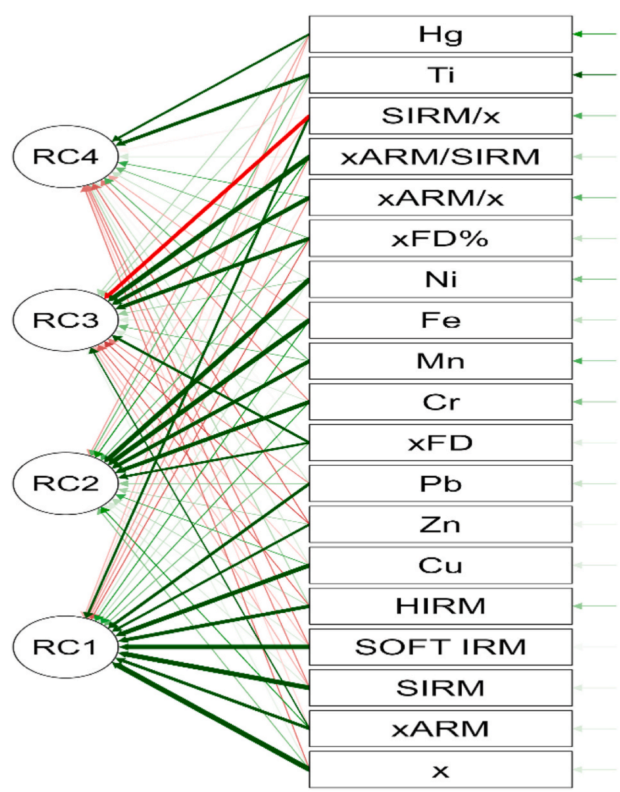

Fig. 8. Path diagram of the Takum top soil.

Table 9
Descriptive statistics of textural parameters in (%) for Takum Town.

Sampling Points	PM 2.5 (%)	PM10 (%)	Clay (%)	Silt (%)	Sand (%)
TRA (n = 08) Range	2.46–12.6	8.85–46.10	4.54–24.28	29.94–71.99	5.01–65.52
Mean ± SD	5.87 ± 3.33	12.25 ± 12.11	11.15 ± 6.43	55.62 ± 16.18	33.23 ± 21.59
CV%	56.70	54.44	57.65	29.08	64.96
TMV (n = 08) Range	1.57–2.64	5.15–9.96	2.73–4.65	17.18–48.77	46.58–79.98
Mean ± SD	1.86 ± 0.37	6.26 ± 1.69	3.16 ± 0.69	28.16 ± 10.93	68.68 ± 11.52
CV%	20.04	27,00	21.98	38.82	16.77
TFL (n = 08) Range	4.50–14.72	17.72–51.18	8.45–28.42	57.18–78.44	1.58–32.77
Mean ± SD	7.18 ± 3.19	28.15 ± 10.70	13.86 ± 6.19	68.28 ± 6.46	19.17 ± 11.29
CV%	44.36	38.00	44.70	9.47	58.92
Total (n = 24) Range	1.57–14.72	5.15–51.99	2.73–28.42	17.18–78.44	1.58–79.98
Mean ± SD	5.19 ± 3.29	19.80 ± 12.05	9.84 ± 6.39	52.36 ± 15.30	38.30 ± 20.68
CV%	63.46	60.84	64.99	29.23	53.99

PM = Particulate Matter.

(Table 9). However, on site specific basis, the sand fraction dominated the TMV unlike TRA and TFL. This suggests higher degree of pedogeneis in the soils around the TRA and TFL over the TMV. This is in agreement with the magnetic grain size result obtained earlier in this study. Larger grains size in TMV over TRA and TFL was found from the χfd% results. Coarser grains size have been associated with industrial pollution (Lu et al., 2007). Higher sand fractions have also been obtained in similar studies by Booth et al. (2007) in Southport, Mersyside, UK, Crosby et al. (2013) in Wolverhampton, UK and Kanu et al. (2019) in Jalingo, Nigeria. The highest mean values of the PM 2.5 and PM 10 are found in the farmland. This might be due to the deposition of products of combustion emanating from an intense and continuous bush burning for farming activities by the inhabitants and vehicular emission particulates from within and long distance sources.

The interrelationships between the particle size classes and magnetic and geochemical parameters obtained via correlation analysis indicated varying strengths and levels of covariation attributed to the varying magnetic and chemical content inherent in each size fraction. The magnetic concentration dependent parameters (χfd, χ, χARM, SIRM, soft IRM, HIRM) showed different degrees of negative correlation with all the particle size classes except the sand fraction (Table 10). Stronger associations are observed with the silt and sand fractions. An almost opposite behaviour is observed in the grain size magnetic parameters (χfd%, χARM/χ and χARM/SIRM) which are positively correlated with the lower size classes (PM2.5, PM10, clay and silt) and negatively correlated with the sand fraction. However, the strength of correlation is weaker ($P < 0.05$) in the grain size parameter than the concentration parameters ($P < 0.05$–0.01). Increase in χfd% with the finer particle size class suggests that the pedogenic magnetic fraction reside in the fine fraction. SP grains are found in the less than 2 μm grades while SD grains are found in the 2–4 μm fraction. The SIRM/χ grain size parameter however followed the trend of the concentration parameters. The SIRM/χ ratio increases with increasing grain size and hence, its positive correlation with the sand fraction. All the magnetic parameters are significantly correlated with the silt and sand fraction. This results implies that the silt and sand fractions are the major carriers of magnetic signals in the Takum soils.

The heavy metal versus particle size correlation shows that Ti, Cr, Mn, Fe, and Cu are significantly positively correlated with sand and negatively correlated with the PM2.5, PM10, clay and silt (Table 10). Ni and Pb followed the same correlation trend. While Pb is poorly correlated with all the textural parameters, Ni display moderate significant negative correlation with PM2.5, PM10 and clay ($P < 0.05$). Hg displayed weak positive correlation with PM2.5, PM10 and clay and poor positive/negative relationship with sit/sand. PM2.5, PM10, clay and sand were poorly negatively correlated with Zn while silt show poor positive correlation with Zn. The relationship between particle size fractions and elemental concentration (just like particle size versus magnetic properties) does not follow a general trend worldwide. Interpretations has to be site specific. Many authors have obtained strong positive correlation between heavy metal and clay fractions (Chen et al., 2016; Aminayanaba and Lawal, 2017). These authors argued that clay has properties such as large surface area and cation exchange capacity that will make them easily absorb and accommodate more heavy metals. This study and several others (Chen et al., 2019; Lin et al., 2021) obtained different trend of correlation. Positive correlation are found between metals and sand fractions as opposed to clay fraction. This suggest that soil textural parameters could not be an effective and recommended proxy for soil heavy metals content.

Table 10
Heavy metals and Textural Parameters correlation matrix for Takum Town. Significant values are bolded.

Variable	PM2.5	PM10	clay	silt	sand
Ti	−0.375	**−0.435a**	−0.383	**−0.681c**	**0.624b**
Cr	**−0.534b**	**−0.558b**	**−0.539b**	**−0.499a**	**0.518b**
Mn	**−0.485a**	**−0.534b**	**−0.491a**	**−0.594b**	**0.579b**
Fe	**−0.447a**	**−0.477a**	**−0.453a**	**−0.425a**	**0.438a**
Ni	**−0.463a**	**−0.481a**	**−0.469a**	−0.337	0.374
Cu	**−0.415a**	**−0.444a**	**−0.42a**	**−0.447a**	**0.448a**
Zn	−0.019	−0.011	−0.017	0.14	−0.108
Hg	0.395	0.353	0.388	0.041	−0.166
Pb	−0.073	−0.086	−0.075	−0.094	0.086
χfd	−0.393	**−0.423a**	−0.403	**−0.486a**	**0.481a**
χfd%	0.232	0.254	0.231	**0.502a**	**−0.461a**
χ	−0.371	−0.403	−0.377	**−0.551b**	**0.528b**
χARM	−0.389	**−0.423a**	−0.399	**−0.530b**	**0.515a**
χARM/χ	0.273	0.288	0.269	**0.494a**	**−0.466a**
SIRM	−0.369	−0.403	−0.376	**−0.555b**	**0.531b**
χARM/SIRM	0.358	0.275	0.255	**0.484a**	**−0.546a**
SIRM/χ	**−0.493a**	**−0.533b**	**−0.5a**	**−0.737c**	**0.715c**
Soft IRM	−0.363	−0.397	−0.37	**−0.549b**	**0.526b**
HIRM	**−0.432a**	**−0.456a**	**−0.436a**	**−0.587b**	**0.583b**

a = $p < 0.05$, b = $p < 0.01$, c = $p < 0.001$.

4. Conclusion

Soil pollution status in Takum topsoil was successfully investigated using multidisciplinary approach. The environmental magnetic approach include measurement of concentration, grain size and magnetic mineral dependent parameters. Magnetic susceptibility values varied from 32.11 to 1118.57 $\times 10^{-8}$ m^3kg^{-1} and SIRM ranged from 199.87 to 16002 $\times 10^{-5}$ Am^2kg^{-1}. This values indicated that there soil have been enhanced due to the presence of secondary ferrimagnetic minerals such as magnetite and maghemite in the soil. The dominance of MD magnetite is confirmed by Curie point temperature of approximately 580 °C obtained from the χ-T curves. This was also supported by the soft IRM and S-ratio, although HIRM revealed that hematite are also present in the soil. The percent frequency dependent susceptibility χfd% had an average value of 10.63% implying that the samples were dominated by pedogenic SP grains, however, the presence of MD grains from vehicular sources were also present in the TMV. The Dearing's plot revealed that the samples were composed of MD, PSD and SSD grain sizes while the Day plot revealed that MD and PSD are the major grain size.

The mean concentration of the heavy metal determined decrease in the order: Fe > Ti > Mn > Zn > Pb > Cu > Ni > Hg. The average content of Ti, Zn, Hg and Pb exceeded the geochemical background concentration by 2.6, 1.3, 20.0 and 2.1 times respectively, implying different levels of anthropogenic influence on the soil. Based on the estimated pollution indices, Pb and Hg constitute the greatest ecological risk in the study area. This calls for concern and further research on these elements should be intensified to ascertain the like sources and mitigation approaches. Various degrees of strong significant positive correlation were obtained between χ, SIRM, χARM, soft IRM and HIRM and Cr, Fe, Zn, Pb and PLI, with χARM having the strongest correlation coefficient. This support the use of environmental magnetic properties for quick assessment and monitoring of pollution levels in the Takum soils. Based on geostatistical analysis, the sources of heavy metal pollution have been identified to originate from vehicular, agricultural, geogenic and weathering activities.

The soil texture in Takum soil was found to consist of 52.36% silt, 38.30% sand and 9.84% clay. The high silt contents implied high pedogenic activities in the soil. The average values of the respiratory health sizes (PM 2.5 and PM 10) are 5.19% and 19.80% respectively. Different degrees of covariation were obtained between magnetic parameters, heavy metals and particle size. The fact that a clear pattern is not obtained from the correlation results of both heavy metals and magnetic parameters and soil texture implied that, care must be taken when attempting to apply magnetic and geochemistry as particle size proxy. There is no general or universal pattern of covariation between these parameters, hence, application has to be on a site specific basis.

Declaration of competing interest

The authors declare that they have no known competing financial interests or personal relationships that could have appeared to influence the work reported in this paper.

Data availability

Data will be made available on request.

Acknowledgement

All the instruments used for this study belongs to the Indian Institute of Geomagnetism (IIG) where the laboratory work was carried out. The authors are deeply grateful to the Director of the Institute and DST, Government of India for granting permission to use the facilities. The first author appreciates TETFund (TETFund/TSU/15/018) for the PhD Bench work grant to IIG.

References

Adie, G.U., Osibanjo, O., 2009. Assessment of soil-pollution by slag from an automobile battery manufacturing plant in Nigeria. Afr. J. Environ. Sci. Technol. 3 (9), 239–250.

Aminayanaba, O.A., Lawal, O., 2017. Investigation of relationship between sediment characteristics and heavy metals across seasons in the Lower Focados River, Nigeria. J. Appl. Sci. Environ. Manag. 21 (1), 208–215.

Angulo, E., 1996. The Tomlinson Pollution Load Index applied to heavy metal,'Mussel-Watch'data: a useful index to assess coastal pollution. Sci. Total Environ. 187 (1), 19–56.

Ayoubi, S., Jabbari, M., Khademi, H., 2018a. Multiple linear modelling between soil properties, magnetic susceptibility and heavy metals in various land uses. Modeling Earth Syst. Environ. 4 (2), 579–598.

Ayoubi, S., Soltani, Z., Khademi, H., 2018b. Particle size distribution of heavy metals and magnetic susceptibilty in industrial site. Bull. Environ. Contam. Toxicol. 100 (5), 708–714.

Ayoubi, S., Adman, V., Yousefifard, M., 2019. Use of magnetic susceptibility to assess metal concentration in soils developed on a range of parent materials. Ecotoxicol. Environ. Saf. 168, 138–145.

Ayoubi, S., Samadi, M.J., Khademi, H., Shirvami, M., Gyasi-Agyei, Y., 2020. Using magnetic susceptibility for predicting hydrocarbon pollution levels in a petroleum refinery compound in Isfahan Province, Iran. J. Appl. Geophys. 172, 103906.

Aziz, K., Ayoubi, S., Nabiollahi, K., Garosi, Y., Gislum, R., 2022. Predicting heavy metal content by applying machine learning approaches and environmental covariates in West of Iran. J. Geochem. Explor. 233 (426), 106921 https://doi.org/10.1016/j.explo.2021.106921.

Barakat, A., El Baghdadi, M., Rais, J., Nadem, S., 2012. Assessment of heavy metal in surface sediments of Day River at Beni-Mellal region, Morocco. Res. J. Environ. Earth Sci. 4 (8), 797–806.

Basavaiah, N., 2012. Geomagnetism: Solid Earth and Upper Atmosphere Perspectives. Springer Science & Business Media.

Basavaiah, N., Khadkikar, A.S., 2004. Environmental Magnetism and its Application towards Palaeomonsoon Reconstruction.

Bender, O.W., Schroeter, R.A., Garcia, M.G., Szente, R.N., 1998. Treating electroplating residues with thermal plasmas. JOM 50 (7), 32–35.

Blaha, U., Appel, E., Stanjek, H., 2008. Determination of anthropogenic boundary depth in industrially polluted soil and semi quantification of heavy metal loads using magnetic susceptibility. Environ. Pollut. 156, 278–289.

Booth, C.A., Winspear, C.M., Fullen, M.A., Worsely, A.T., Power, A.L., Holden, V.J.C., 2007. A pilot investigation into the the potential of mineral magnetic measurements as a proxy for urban roadside particulate pollution. In: Borrego, C.A., Brebbia, C.A. (Eds.), Air Pollution XV. WIT Press, Ashurst, pp. 391–400.

Cai, L.M., Wang, Q.S., Wen, H.H., Luo, J., Wang, S., 2019. Heavy metals in agricultural soils from a typical township in Guangdong Procince, China: occurrences and spatial distribution. Ecotoxicol. Environ. Saf. 168, 184–191.

Carter, J.D., Barber, W., Tail, E.A., 1963. The geology of parts of Adamawa, Bauchi and Bornu Provinces in Northeastern Nigeria. Bull No. 30 Geological Survey of Nigeria 108.

Chaparro, M.A.E., Sinito, A.M., Ramasamy, V., Marinelli, C., Chaparro, M.A.E., Mullainathan, S., Murugesan, S., 2008. Magnetic measurements of pollutants of sediments from Cauvery and Palaru river, India. Environ. Geol. 56, 425–437.

Chaparro, M.A.E., Chaparro, M., Cordoba, F.E., Lecomte, K.L., Gargiulo, J.D., Barrios, A. M., Uran, G.M., Manograsso, C.N.T., Lavat, A., Bohnel, H.N., 2017. Sedimentary analysis of magnetic properties of lake Anonima, Vega Island. Antarct. Sci. 29 (5), 429–444.

Chen, T., Liu, X., Li, X., Zhao, K., Zhang, J., Xu, J., Shi, J., Dahlgren, R.A., 2009. Heavy metal sources identification and sampling uncertainty analysis in a field-scale vegetable soil of Hangzhou, China. Environ. Pollut. 157 (3), 1003–1010.

Chen, Y., Gao, J., Yuan, Y., Ma, J., Yu, Su, 2016. Relationship between heavy metal contents and clay mineral properties in surface sediments: implications for metal pollution assessment. Continent. Shelf Res. 124, 125–133. https://doi.org/10.1016/j.csr.2016.06.002.

Chen, F., Chen, X., Zhu, F., Sun, Q., 2019. Study on the factors affecting the spatial distribution of heavy metal elements, 2019 IOP Conf. Ser. Earth Environ. Sci. 330, 042013. https://doi.org/10.1088/1755-1315/330/4/042013.

Crosby, C.J., Booth, C.A., Fullen, M.A., 2013. Mineral magnetic measurements as particle size proxy for urban roadside soil pollution (part 1). Environ. Sci. Process Impacts. https://doi.org/10.1039/c3em0 03446b.

Dankoub, Z., Ayoubi, S., Khademi, H., Lu, S.G., 2012. Spatial distribution of magnetic properties and selected heavy metals in calcareous soils as affected by land use in the Isfahan Region, Central Iran. Pedosphere 22 (1), 33–47. https://doi.org/10.1016/S1002-0160(11)60189-6.

Das, P.K., 2014. Magnetic Investigations of Urban Pollution at Mumbai and Nashik, Maharashtra, India: Mineral Magnetic Method as a Pollution Proxy, PhD Thesis. University of Mumbai, p. 205.

Dearing, J.A., Hay, K.L., Baban, S.M.J., Huddleston, A.S., Wellington, E.M.H., Loveland, P., 1996. Magnetic susceptibility of soil: an evaluation of conflicting theories using a national data set. Geophys. J. Int. 127 (3), 728–734.

Dearing, J.A., Bird, P.M., Dann, R.J.L., Benjamin, J.F., 1997. Secondary ferrimagnetic minerals in Welsh Soils: a comparison of mineral magnetic detection methods and implications for mineral formation. Geophys. J. Int. 130, 727–736.

Dickinson, W.W., Dunbar, G.B., McLeod, H., 1996. Heavy metal history from cores in Wellington Harbour, New Zealand. Environ. Geol. 27 (1), 59–69.

Dong, C., Zhang, W., Ma, H., Feng, H., Lu, H., Dong, Y., Yu, L., 2014. A magnetic record of heavy metal pollution in the Yangtze River subaqueous delta. Sci. Total Environ. 4766 –477, 368–377.

Evanhoe, R., 2006. Metal pollution from medieval mining persists. Chemical and Engineering News of August 17, 2006.

Evans, H.E., Heller, F., 2003. Environmental Magnetism, Principles Aand Applications of Environmegnatics, International Geophysical Series, 86. Academic Press, p. 299.

Guda, A.M., El-Hamaly, L.A., Abdel Aal, E.M., Odah, H., Appel, E., El Kammar, A.M., Abu Khatita, A.M., Abu Salem, H.S., Awad, A., 2020. Suitability of magnetic proxies to reflect complex anthropogenic spatial and historical soil heavy metal pollution in southeast Nile delta. Catena 191, 104552. https://doi.org/10.1016/j.catena.2020.104552.

Guo, W., Huo, S., Ding, W., 2015. Historical records of human impact in a lake of northern China: magnetic susceptibility, nutrients, heavy metals and OCPs. Ecol. Indicat. 57, 74–81.

Hakanson, L., 1980. An ecological risk index for aquatic pollution control. A sedimentological approach. Water Res. 14 (8), 975–1001.

Hartley, W., Dickinson, N.M., Clemente, R., French, C., Piearce, T.G., Sparke, S., Lepp, N. W., 2009. Arsenic stability and mobilization in soil at an amenity grassland overlying chemical waste (St. Helens, UK). Environ. Pollut. 157 (3), 847–856.

ISO 21226:2019 Soil Quality, 2019. Guidelines for the Screening of Soil Polluted with Toxic Elements Using Soil Magnetometry.

Iwegbue, C.M.A., Egobueze, F.E., Opuene, K., 2006. Preliminary assessment of heavy metals levels of soils of an oil field in the Niger Delta, Nigeria. Int. J. Environ. Sci. Technol. 3 (2), 167–172.

Iyama, W.A., Okpara, K., Techato, K., 2022. Assessment of heavy metals in agricultural soils and plant (*Veronia amygdalina delile*) in Port Harcourt Metropolis, Nigeria. Agriculture 12, 27, 10.390/agriculture 12010027.

Jiang, H.H., Cai, L.M., Wen, H.H., Hu, G.C., Chen, L.G., Luo, J., 2019. An integrated approach to quantifying ecological and human health risks from different sources of soil heavy metals. Sci. Total Environ. https://doi.org/10.1016/j.scitotenv.2019.134466.

Kanu, M.O., Meludu, O.C., Oniku, S.A., 2013. Magnetic susceptibility of soils in Jalingo, N-E Nigeria:A cas study of the Jalingo mechanic village. World Appl. Sci. J. 24 (2), 178–187. https://doi.org/10.5829/idosi.wasj.2013.24.02.13173.

Kanu, M.O., Basacaiah, N., Meludu, O.C., Oniku, S.A., 2017. Investigating the potential of using Environmental magnetism techniques as pollution proxy in urban deposited road sediment. Int. J. Environ. Sci.Tech. 14, 2745–2758. https://doi.org/10.1007/s13762-027-1356-5.

Kanu, M.O., Meludu, O.C., Basavaiah, N., Oniku, A.S., 2018. In: Rabiu, A.B., Abiye, O.E. (Eds.), Magnetic and Metal Pollution Studies of Topsoils from Residential Areas of Jalingo Metropolis, Taraba State, N-E Nigeria, Monograph of Atmospheric Research. Centre for Atmospheric Research, Anyibga, Nigeria, pp. 92–102.

Kanu, M.O., Meludu, O.C., Basavaiah, N., Oniku, A.S., 2019. Relationship between mineral magnetic properties and soil textural parameters. Acta Geophys. https://doi.org/10.1007/s11600-019-00248-8.

Karimi, R., Ayoubi, S., Jalalian, A., Sheikh-Hosseini, A.R., Afyuni, M., 2011. Relationship between magnetic susceptibility and heavy metals in urban topsoils in the arid region of Isfahan, Central Iran. J. Appl. Geophys. 74 (1), 1–7. https://doi.org/10.1016/jappgeo.2011.02.009.

Lin, J., Sadique Rayhan, A.B.M., Wang, Y., Wu, Zhai, Lin, Y., Ke, H., Li, T., Chen, K., Cai, M., 2021. Distribution and contamination assessment of heavy metals in soils and sediments from the Fildes Peninsila and Aedley Island in king George Island, Antarctica. Polar Res. 40, 5270. https://doi.org/10.33265/polar.v40.5270.

Liu, Q., Roberts, A.P., Torent, J., Horng, C.S., Larransoana, J.C., 2007. What do the HIRM and Sratio really measure in Environmental magnetism? G-cubed 8, Q09011. https://doi.org/10.1029/2007GC001717.

Liu, Q., Roberts, A.P., Larrasoana, J.C., Baherjee, S.K., Guyodo, Y., Tauxe, L., Oldfield, F., 2012. Environmental magnetism: principles and applications. Rev. Geophys. 50, RG4002. https://doi.org/10.1029/2012RG000393.

Lu, S.G., Bai, S.Q., Xue, Q.F., 2007. Magnetic properties as indicators of heavy metals pollution in urban topsoils: a case study from the city of Luoyang, China. Geophys. J. Int. 171, 568–580.

Lu, S., Wang, H., Guo, J., 2010. Magnetic Response of Heavy Metals in Urban Soils: Magnetic Proxy Parameters as an Indicator of Heavy Metals Pollution, 19th World Congress of Soil Science, Soil Solutions for a Changing World, 1-6 August, 2010, Brisbane, Australia.

Lyu, S., Wei, X., Chem, J., Wang, C., Wang, X., Pan, D., 2017. Titanium as a beneficial element for crop production. Front. Plant Sci. 8, 597. https://doi.org/10.3389/fpls.2017.00597.

Maher, B.A., 1988. Magnetic properties of some synthetic submicron magnetites. Geophys. J. 94, 86–96.

Manisalidis, I., Stavropoulou, E., Stavropoulos, A., Bezirtzoglou, E., 2020. Environmental and health impacts of air pollution: a review. Front. Public Health 8, 14. https://doi.org/10.3389/fpubh.2020.00014.

Matini, L., Ossebi, J.G., Mbedi, R., Moutou, J.M., 2012. Rare earth elements in soil on spoil heap of an abandoned lead ore treatment plant in the District of Mfouati , Congo-Brazzaville. Int. Res. J. Environ. Sci. 1 (2), 33–40.

Naderizadeh, Z., Hosseni, K., Ayoubi, S., 2016. Biomonitoring of atmospheric heavy metals pollution using dust deposited on date palm leaves in Southwestern Iran. Atmósfera 29 (2), 141–155. https://doi.org/10.20937/ATM.2016.29.02.04.

Nur, A., Goji, M., 2005. Hydro-geological study in Takum and Environs of Taraba state, NE Nigeria. Global J. Geol. Sci. 3 (2), 109–115.

Oldfield, F., 1991. Environmental magnetism—a personal perspective. Quat. Sci. Rev. 10 (1), 73–85.

Oruson, M.M., Oniku, S.A., Peter, A., Orosun, R.O., Salawu, N.B., Hitler, L., 2020. Magnetic susceptibilty and heavy metal pollution at automobile station, Illorin, north-Central, Nigeria. Environ. Res. Commun. 2, 015001 https://doi.org/10.1088/2515-7620/ab636a.

Oyeleke, P.O., Abiodun, O.A., Salako, R.A., Odeyemi, O.E., Abejide, T.B., 2016. Assessment of some heavy metals in the surrounding soils of an automobile battery factory in Ibadan, Nigeria. Afr. J. Environ. Sci. Technol. 10 (1), 1–8.

Pobi, K.K., Satpati, S., Dutta, S., Nayek, S., Saha, R.N., Gupta, S., 2019. Sources evaluation and ecological risk assessment of heavy metals accumulated within a natural stream of Durgapur industrial zone, India, by using multivariate analysis and pollution indices. Appl. Water Sci. 9–58. https://doi.org/10.1007/s13201-019-0946-4.

Rudnick, R.L., Gao, S., 2014. 4.1- Composition of the continental crust. In: Holland, H., Turekian, K. (Eds.), Treatise on Geochemistry, second ed. Elsevier, Oxford, pp. 1–51. https://doi.org/10.1016/B978-0-08-095975-7.00301-6.

Singh, A.K., Hasnain, S.I., Banerjee, D.K., 1999. Grain size and geochemical partitioning of heavy metals in sediments of the Damodar River–a tributary of the lower Ganga, India. Environ. Geol. 39 (1), 90–98.

Soodan, R.K., Pakade, Y.B., Nagpal, A., Katnoria, J.K., 2014. Analytical techniques for estimation of heavy metals in soil ecosystem: a tabulated review. Talanta 125, 405–410.

Sutherland, R.A., 2000. Bed sediments associated trace metals in urban streams, Oahu, Hawaii. Environ. Geol. 39, 611–627.

Taghipour, M., Ayoubi, S., Khademi, H., 2011. Contribution of lithogenic and anthropogenic factors to surface soil heavy metals in Western Iran using multivariate geostatistical analyses. Soil Sediment Contam.: Int. J. 20 (8), 921–957.

Teng, D., Mao, K., Ali, W., Xu, G., Huang, G., Niazi, N.K., Feng, X., Zhang, H., 2020. Describing the toxicity and sources and the remediation technologies for mercury - contaminated soils. RSC Adv. 10, 23221.

Tomlinson, D.L., Wilson, J.R., Harris, C.R., Jeffrey, D.W., 1980. Problems in the assessment of heavy metals levels in estuaries and the formation of a pollution index. Helgol. Wiss. Meeresunters. 33, 566–575.

Van Oorschot, I.H.M., 2001. Chemical Distinction between Lithogenic and Pedogenic Iron Oxides in Environmental Magnetism, A Search for the Perfect Solution. PhD thesis submitted to. University of Utrecht, p. 185. No. 208.

Verosub, K.L., Roberts, A.P., 1995. Environmental magnetism: past. present and future. J. Geophys. Res. 100, 2175–2192. https://doi.org/10.1029/94JB02713.

Wang, G., Zhang, S., Xiao, L., Zhong, Q., Li, L., Xu, G., Deng, O., Pu, Y., 2017. Heavy martals in soils from a typical industrial areas in Sichuan, China: spatial distribution, Source identification and ecological risk assessment. Environ. Sci. Poll. Res. 24 (20), 16618–16630.

Wang, L., Hub, S., Yub, G., Mab, M., Wang, Q., Zhang, Z., Liao, M., Yeb, L., Wang, X., 2018. Magnetic characteristics of sediments from a radial sand field in South Yellow sea, Eastern China and environmental implications during the mid-to late –Holocene. J. Asian Earth Sci. 163, 224–234. https://doi.org/10.1016/j.jseaes.2018.05.035.

Weissmannova, H.D., Cova, S.M., Chovanec, P., Pavlovsky, J., 2019. Potential ecological risk and human health risk assessment of metal pollution in industrial affected soils by coal mining and metallurgy in Ostrava, Czech Republic. Int. I. Environ. Res. Public Health 16, 4495. https://doi.org/10.3390/ijerph16224495.

WHO, 1982. Titanium, 24. Environmental Health Criteria.

Yamada, D., Hiwatari, M., Hangoma, P., Narita, D., Mphuka, C., Chitah, B., Yabe, J., Nakayama, S.M.M., Nakata, H., Choongo, K., Ishizuka, M., 2020. Assessing the population-wide exposure to lead pollution in Kabwe, Zambia: an econometric estimation based on survey data. Sci. Rep. 10 (1), 1–11. https://doi.org/10.1038/s41598-020-71998-5.

Yang, T., Liu, Q., Li, H., Zang, Q., Chan, L., 2010. Atmospheric magnetic particles and heavy metals in the road dust: magnetic identification and its implications. Atmos. Environ. 44, 1175–1185.

Yang, D., Wang, M., Lu, H., Ding, Z., Liu, J., Yan, C., 2019. Magnetic properties and correlation with heavy metals in mangrove sediments, the case study on the coast of Fujian, China. Mar. Pollut. Bull. 146, 865–879.

Zao, D., Wu, Q., Zheng, G., Zeng, Y., Wang, A., Gao, S., Zhang, Y., 2022. Quantitative source apportionment and uncertainty analysis of heavy metal(loids) in the top soil of the Nansi Lake Nature Reserve. Sustainability 14, 6679. https://doi.org/10.3390/su1416679.

Zhang, F.S., Li, Y.X., Yang, M., Li, N., 2012. Content of heavy metals in animal feeds and manures from farms of different scales in northeast China. J. Environ. Res. Public Health 9, 2658–2668.